1. CHAPTER 1: INTRODUCTION

The study was carried to analyze the behavior of process parameters on weld strength of Friction Stir Welding numerically. This work will be performed into two steps; at First, numerical simulations on thin sheets for similar material will be performed by using experimental data to observe the influence of process parameter on tensile strength. Then similar simulations will be done to analyze the behavior of parameters on thick sheets for dissimilar materials as well.

1.1 Aims and Objectives:

The purpose of study is to consider optimal values of basic parameters that influence weld strength for FSW of Al alloy. Modeling and simulation of FSW for thin and thick sheet will validate the experimental data by providing precise and accurate results.

The main objectives are defined as:

- To model, analyze and distinguish suitable parameters that affect weld strength of similar and dissimilar materials by using experimental data.
- ABAQUS/CAE commercial software would be used for modeling and simulation of data.

1.2 Motivation of Research:

Friction stir welding exceeds among other welding techniques because of its mechanical properties such as high joint strength, less defective and low distortion. Initially Friction Stir Welding was observed for Aluminum alloys but with time it has emphasized on accommodating other softer materials and low temperature alloys for better quality welds. [13] Many Researchers have observed the behavior of parameters theoretically, also numerical simulations were also done but there is a lot more to be done [5].

1.3 Research Layout

This study will be performed in different steps. Firstly mechanical properties of materials will be obtained. Then consideration of appropriate software for modeling is done.

Different boundary conditions and meshing tools will be observed. At end simulation results will be compared with experimental results to validate them. Research scheme for this study is exhibited in figure 1.1.

Modeling & Validation of Friction Stir Welding

1. FSW of similar alloys on thin sheet

- Finalizing of process parameters affecting weld strength of FSW on thin sheets
- Optimization of material properties
- Literature Review

2. Modeling of Experimental data

- Choosing Appropriate software
- Consideration of Boundary Conditions & Material properties
- Finalizing model of tool and plates
- Geometry Formation

3. Meshing and Boundary Conditions

- Application of BCs for particular rotational speed and traverse speed
- Meshing of model

4. Simulation & Validation

- Simulations for nine experiments will be done.
- Results will be compared with experimental data

5. FSW of dissimilar alloys on thick sheets

- Similar procedure will be adopted for dissimilar alloys for thick sheets
- Observation of influence of process parameters on weld strength
- Validation of Model

1.4 Thesis overview:

This study has been distributed into different chapters. Each chapter elaborates different contents. This research is performed in similar pattern as described below.

1.4.1 Chapter 2 Literature Review:

In this chapter, brief description of Friction stir welding is discussed obtained from literation. Also different new techniques introduced for modeling in past years is described.

1.4.2 Chapter 3 Methodology

Data obtained from experiments is considered and appropriate software for modeling and simulation of experimental data is discussed. Different meshing conditions, boundary conditions and mechanical properties required for simulations are observed.

1.4.3 Chapter 4 Results and discussions

Results obtained during simulating experimental data for similar and dissimilar materials are analyzed. Stress strain curve obtained for each material is examined and comparison is done with experimental data to validate the results

1.4.4 Chapter 5 Conclusions & Future work

This chapter will propose conclusion observed from result and suggestions for future work required in this study.

CHAPTER 2: LITERATURE REVIEW

2.1 Introduction of Welding Processes:

The method of joining materials, such as metals and polymers at higher temperature is called welding. Thus materials to be joined are melted along their interface and addition of filler occurs which creates pool of molten materials that coagulates into firm joint. The ability to attain perfect structure strength by welded into permanent joint is termed as weldability. It is dependent on five major factors; melting point, thermal conductivity, thermal expansion, surface condition and external environment [4].

Welding has major contributions in fabrication of auto mobile bodies, structural work, tanks, repairing of parts; it is also employed in various industries, refineries and also for manufacturing of pipe lines. Being cost efficient, it has expelled from other joining processes as heat is obtained electrically or by using gas torch.

2.1.1 Advantages of Welding:

Welding is termed as important fabrication process as efficiency of metals can be observed by their tendency to be welded. Advantages of Welding that exceeds it from other joining techniques are given below:

- As Compare to other joining process, structures and parts fabricated by welding are less in weight
- Joint manufactured by welding have attained strength.
- Rivets and bolts joints are less corrosion resistant as compare to welding joints.
- Welding is capable of producing strong joints in less time; also it is less noise is produced.
- Moreover welding is termed as least expensive process and requires less working space.

2.1.2 Classification of welding process:

Welding is usually classified into three major types i.e. Solid State Welding, Fusion Welding and Soldering and brazing. Welding process in which intimate contact occurs between two materials by applying pressure and heat at a temperature below their melting point is termed as solid state

welding. Solid State Welding has been classified into various types which may include some old techniques and some are newly introduced. [16]

While in soldering and brazing at lower melting temperature, materials are joined together without melting them. Brazing joints are considered to stronger than soldering as they may join dissimilar materials as well. Both Soldering and Brazing requires Flux in order to attain clean metal surfaces. Both Soldering and Brazing are considered in between Fusion and Solid State Welding. [4]

In fusion Welding two materials are fastened by heating them to melting point. It does not involve the use of Filler material. Fusion welding plays a major contribution in fabrication of different parts [17].

2.2 History of Friction Stir Welding:

This technique was developed by The Welding Institute (TWI) in December, 1991 [1]. Since discovered, this process is widely used worldwide for higher production projects and research in various fields i.e. industries, automotive, aerospace, ship building, electrical appliances and heat exchangers. FSW is considered to be revolutionary discovery because it is capable of incorporating various materials such as aluminum, brass, copper and other low melting material by maintaining their mechanical properties. Friction Stir welding is a method in which heat is generated by friction between stationary and moving part [14]. The process was initially subjected for aluminum alloys but later this process was also employed for softer materials. The main risk during this process is false tppl degradation due to high stress and temperature at stir zone, which causes FSW challenging for commercial use because of higher tool cost [1]. FSW is a process in which different materials are joined without melting. Mixing of material for homogenous weld and generation of plasticized conditions are major aspect of FSW. Moreover by stimulating plasticized material of welding corners with rotating pin pushed into material and moving along joint line cause the joining of welded material [2].

Due to its energy efficiency, Friction Stir Welding is labeled as Green Technology. Weld quality is dependent on welding parameters and tool geometry; this also plays vital effect on temperature distribution. [12]

2.3 Applications of FSW:

Friction stir welding technique is used worldwide because of its tremendous applications in the field of aerospace, auto motives and ship building. [14]. Advantages of Friction Stir welding are described in Table 2-1.

Table 2-1: Benefits of Friction Stir Welding [15]

Metallurgical Advantages	Environmental Advantages
1. Low distortion occurs during FSW.	1. Post cleaning is not needed
2. Welded plates have good dimensional accuracy	2. Flux and shielded gas are not required
3. No cracking and material loss occurs	3. Helps to utilize material, thus no wastage of material
4. Material has gained excellent mechanical properties	4. Elimination of wastes
5. Can weld both similar and dissimilar alloys	5. It helps in reducing need of solvents

2.4 Past work on Friction Stir welding:

2.4.1: Effect of Parameters:

Aluminum alloy is widely utilized in manufacturing of light weight structures for providing high strength to weight ratio. In friction Stir Welding, material used for welding does not melt and recast. Tool used to provide frictional heat remains non consumable. The purpose is to analyze the behavior of welding speed and tool pin profile on FSW using aluminum alloy. Different types of tool pin are employed to generate joints at three different welding speeds. Aluminum alloy used is 300mm*150mm in size; plates are of 6mm thickness. Usually in fusion welding process many defects such as porosity, slag including cracks occur while process of FSW is defect free. The joints formed during this process are observed at low magnification using optical microscope. From results it was observed that square pin profiled tool produce defect free FSP region and welding speed of 0.76mm/s showed superior properties than other welding speed.

Among 15 joints, joints used by square pin at 0.76mm/s gave better tensile strength, higher hardness and finer grains in FSP region [11].

Due to difference in temperature characteristics of material, aluminum welding cannot be subjected to convectional process. Friction Stir Welding is done to reduce such problems. Two plates or sheets of Al are joined together and required cylindrical tool with threaded profile for this process. Usually in FSW, welding of Al will take place without changing its properties thus providing better surface finish and high quality parameters such as axial force, rotation speed, transverse speed and tool tilt angle. FSW is performed on AA 6082 alloy weld plates. For better quality weld rotation speed of 1000-12000 rpm is done. Tensile test has been performed which revealed that tensile strength is minimized by only 10% of base metal. Tensile properties are enhanced by increasing rotation speed [4].

For better weld strength and microstructural properties, polycrystalline combine boron nitride and tungsten alloys made FSW applicable on stainless steel, hardened steel and super alloy. Basically in FSW, non-consumable tool of harder material than work piece is used for joining different materials, fixed into joint line while tool is moving along two clamped plates. For high efficient joint, tool is considered to be an important and critical component. Hardness of work piece material has major contribution in selection of tool material; however it must qualify following parameters such as resistance to creep, dimensional stability, resistant thermal fatigue, resistant to failure etc. [1].

2.4.2 Residual Stresses in FSW

As compared with other welding process, residual stress in FSW is lower. For the analysis of transient temperature and residual stresses numerical simulation is done in two stages. In the first stage, thermal behavior of piece was observed and generation of heat due to friction between tool and work piece. While in second stage this thermal behavior is used to analyze the residual stresses in model. Friction Stir Welding consists of two plates plunged into another plate. Tool moves lower towards plates until shoulder touches the surface of tool. Due to spinning, heat occurs due to friction as a result tool moves onto plate and strong joint is formed. For better joint tool's position is angled at certain direction. During welding thermal stress occurs while during cooling expansion and contraction of material is formed. After complete cooling of plate,

residual thermal stresses are observed. From results it can be observed that experimental results are lower than predicted value. [10]

2.4.3 Numerical Modeling:

Thus numerical modeling is done to analyze behavior of welding tool and thermal distributions. Boundary conditions and general features are taken into account for tool modeling while for thermal analysis two modes are considered i.e. stable and unstable heat input. Two dimensional model of tool is created in Pro Engineer. This model is shifted to ANSYS for thermal analysis using quadrilateral elements. The thermal conductivity of tool is considered to be 28W/m-K. Almost six types of meshing is performed within range of 464 to 5153 nodes. Mixed boundary conditions are observed for part of tool towards environment while for cooled tool holder temperature is kept constant. This will give total heat input in order to analyze different the reaction of process parameter, this is the function of operating parameters. Results predicted that varying heat input is incurred at shoulder periphery i.e. 79% while tool at the base of pin has 20% while pin has 1%. [12]

For Al 6061 and Al 7475, FEA analysis is done at varying speed using ANSYS. Numerical model will be created in Pro Engineer at speeds of 800 rpm, 650 rpm and 450 rpm. For deformation, stress and strain determination, static analysis is done while for heat flux and temperature distribution thermal is conducted. The dimensions of plates are same i.e. 100mm * 50mm *5mm with shoulder diameter of 20mm, pin diameter of 2mm and height of 4.7mm. After modeling in Pro Engineer, FEA analysis is done in ANSYS. From results obtained by structural analysis, Stress increases with speed. These plates are created experimentally by CNC machine at 750 rpm with circular tool. After that this plate was passes through various tests i.e. tensile testing, hardness test and impact test. By increasing speed tensile speed increases, hardness decreases while it impact more at high speed that's why 750 rpm is considered as optimal speed.[14]

Friction Stir Welding is considered as revolutionary technique when compared with Fusion Welding Process. Aluminum alloy is used in this process due to its light weight and high strength to weight ratio. The influence of welding and tool pin profile i.e. straight cylindrical and tapered cylindrical is tested for Al 6061. Milling machine is used to perform experiments with

parameters i.e. cutting feed and spindle RPM. For modeling plates of 100mm*50mm*3mm and shoulder radius of 20, pin radius of 2.5 and pin height of 3mm also tool travel rate of 90mm/min and speed of 1200 rpm was taken. For numerical modeling Pro engineer is used. At 1200 rpm Al alloy consists of temperature 703K and pressure of 19.68 MPa. Thermal analysis was done for round tool and round tapered tool. For analysis ANSYS software was used. With increase in Rpm, temperature, heat flux and temperature gradient increases. Temperature gradient and flux for round taper tool is high while welding characteristics of round tool seems better [13]

To perform computations moveable cellular automation method is adopted. Two types of simulations were performed. Results show that weld porosity was reduced by frequency and additive ultrasonic vibrations of special amplitude. Also overheating of joining material is avoided by using FSW region. For minimum number of defects ratio of rotational velocity to welding speed must be within interval of 20-40. After that 3D model was adopted which showed that for transporting welded material around pin optimal proportion of rotational and velocity to welding speed must be considered also pins of different shapes must be used this may result in better stir of welded material.[2]

Hemispherical punch stretching method was used for investigation of formability of AA-7075-T6 friction stir welded tailor made plate. This also involves the analysis of effect of welding process and deformation temperature on formability. When forming occurs at high temperature, formability material also increases. To predict the onset falling three different localized necking models were adopted through numerical simulation. FLDs of base and Friction stir weld can also be analyzed by Tresca Criterion. Metals sheet are fabricated by welding together in tailor welded blanks. Prediction of forming limits is vital because welding causes some defects and fracture in material. To generate TWBs aluminum sheet of 1-2mm thickness was analyzed. Field emission scanning electron microscope was operated to examine fracture surface. Due to plastic deformation and increased temperature, mechanical properties of material must be varied. By taking in account various properties, nine regions were introduced. Thin sheets of aluminum were joined by FSW. Almost three failure criteria were adopted to analyze failure limits. Tresca model was used to calculate formability limits of base material at room temperature. [3]

Research carried on FSW of aluminum has led to emphasize on FSW of steel and other high melting temperature alloys. For cost effective FSW of steel, numerical modeling has been carried

out. For modeling of FSW of steel, Coupled Eulerion Lagragian approach is applied. Comparing with previous results, weld shape and weld surface flash were considered to be exceptional in each model. For calculation of thermal and structural representation of model, fully coupled thermal and structural displacement approach is considered. For better results, temperature dependent properties like coefficient of thermal expansion, thermal conductivity and specific heat were used. Insignificant flash is produced during first weld metal due to maximum rotation and translation of tool. Eulerion Lagragian approach successfully estimated temperature distribution, plastic strain and flash generation in all three stages i.e. plunge, dwell and transverse in workpiece. The process is seen to be realistic, because no modifications were observed in both models.[5]

To reduce fixtures issue in fusion of thin sheet, simple mechanical fixture is used. This fixture resembles to a lever type clamp and it is capable of holding thin sheets close to weld line precisely. Asbestos is used as cover plate to reduce heat loss. This is done by welding of 0.5mm thin Al alloy 6061-T6 sheets positioned at distinct tool travel speed. From the macrostructure it can be predicted the TMAZ decrease with tool travel speed. Weld similar shape to saddle is considered. Work piece material is softened due to friction produced between tool and work piece in FSW process. The rotating tool will thus deform the two work pieces and joined is produced. Thinning and excessive flash does not occur as rise of thin sheets ahead of tool was reduced by clamping sheets. This welding occurred at speed of 150-200mm/min and radius of curvature between TMAZ and HAZ was increasing with expansion of tool travel speed, defects were also observed close to ^{high} travel speed and falling of UTS [6].

For joint formation of 0.5mm thin Al 60-61 sheet plunging depth of 0.05mm was taken by micro. FSW area of load bearing was enhanced by attaining minimum ratio of thickness reduction of 2%. By lowering and increasing plunging depth relative to 0.05mm, defect such as groove, flash and also reduction in thickness will occur. Surface appearance is enhanced by increasing rotational speed. In correspond to welding tool 1, welding tool 2 will produce stirring at increased tool strength of 217 MPa was achieved. [7]

By changing rotational speed, result of grain size, grain orientation and precipitates on mechanical properties of FS welded 5A06 Al alloy was analyzed. Usually recrystallization takes place at weld zones and shear texture components with higher rotational speed are used in place

of recrystallization texture components. Coarsing of grains at increasing rotational speed will cause generation of shear texture, precipitates relationship dissolution and dislocation. In Hal-Petch relationship, the consequence of grain size hardness is constant throughout. In arc welding defect such as welding porosity and hot cracking are caused which are neglected in FSW. Moreover it generates finer grain size, no smoke, no smoke, no pores, no flash as compare to traditional welding. Aluminum alloy 5A06 of thickness 5.17mm is used. Shoulder of 15mm dia and produce tilted $1^{o}58'$ with root dia of 5.8mm, tip dia of 3.5mm and length of 4.7mm was considered. To calculate mechanical properties of welds, tensile test and Vickers hardness tests are considered. Impact of grain size is more effective on hardness distribution rather than influence of precipitate. [8]

Using the technique of FSW, aluminum alloy plate is welded to a mild plate and effect of pin rotation speed and position of pin on tensile strength and microstructure of joint was investigated. This also helped to observe the behavior of oxide on faying surface. Fracture part of joint shows the presence of intermetallic compounds in that region. It is possible to eliminate oxide film from faying surface by rubbing motion of rotating pin. With time the fabrication of vehicles is increased by using steel and aluminum together. For experiments rotating pin is fixed into aluminum, this pin is further pushed into faying surface of steel, thus removing oxide film from faying surface. Heat occurred by friction of rotating tool shoulder, which resulted in joining of steel and Al plates. Shoulder of 15cm dia with pin of 2mm diameter and length of 19mm was taken. Rotational speed was optimized up to 100-1250rpm. Intermetallic compound were obtained during steel and aluminum alloy. Presence of intermediate compound resulted into decrease of joint strength. Rubbing motion of rotation pin will result in removal of oxide film from faying surface [9].

2.5 Tool geometry and Operating parameters:

Friction Stir Welding is reflected as the most prominent metal fusing process. Aluminum and other alloys can be easily combined during Friction Stir Welding. Different welding processes consist of parameters which act as fundamental during material joining. In the case of Friction Stir Welding, tool geometry and welding process parameters are assumed essential during fabrication of materials.

Tool geometry composed of two major parts i.e. tool shoulder and pin, which are considered as critical needs during FSW. Tool performs two important tasks which are localized heating and material flow. In the first task, heat occurs due to abrasion between pin and work piece. Deformation of material also extracts some heat. Friction between pin and shoulder are important for heat production during FSW. While the other task of material flow have evolved due to revolutionary development in tool shapes and shoulder profiles.

Welding parameters are further classified into two types; rotational speed which occurs due to coagulation of material along pin, it can move in both directions i.e. clockwise and anticlockwise while the other type traverse speed occurs along joint, it helps to translate material back and forth along joint. Apart from these, tilt angle plays an important role. Angle of spindle helps shoulder to manage material along pin efficiently to reduce distortion [15].

For this study, rotational speed, traverse speed, tool shoulder diameter, pin diameter, pin height and probe shapes were considered. These parameters assumed to have greater influence on weld strength and can easily be varied according to requirements.

CHAPTER 3 METHODOLOGY

This chapter will illustrate the theoretical background of experimental data; also it will suggest appropriate software and technique used for simulating experimental results. Optimization can be defined as method to evaluate operating techniques for particular process. Usually hit & trial method is considered to obtain required design [18].Various tools and techniques are used for optimization. In this case simulations are used to evaluate, analyze and validate experimental data. [19]

3.1 Theoretical Background

Previous study investigated the behavior of probe shape in friction stir welding of thin sheet. Utilizing Aluminum Al 5052 as the base material and Taguchi L9 orthogonal array for optimization, three main process parameters; rotational speed, probe shape and traverse speed were discussed with the scope to expand tensile strength. Joints are produced for the rotational speed of 2000 rpm, 2500 rpm and 3000 rpm, traverse speed of 100mm/min, 200mm/min and 400mm/min, tool shape of square, triangle and circle. The results designated square shaped tool as defect free and high strength joints and optimal parameters found are 3250 rpm, 200 mm/min and square shape to produce defect free joint.

Aluminum 5052 H-32 was considered for the study. It has light weight, low maintenance, cold formability, good weldability and excellent corrosion resistance. Properties of Base metal are given in Table 3-1;

Table 3-1: Mechanical properties of Al 5052

Properties	Values
Density	2.68 g/cm^3
Melting Point	605˚ C
Thermal Expansion	$23.7 * 10^{-6}$ /K
Modulus of Elasticity	70 GPa
Thermal Conductivity	138 W/m*K
Electrical Resistivity	$0.0495 * 10^{-6}$ Ω.m

Three parameters were considered for the study to observe their influence on tensile strength; rotational speed, traverse speed and probe shape (circle, square, triangle). After experimentation,

nine samples were analyzed to determine their tensile, hardness and microstructure properties by Taguchi methodology [20].

3.2 Modeling & Simulation of Experimental data:

For modeling experimental data, appropriate software is required. For this purpose, initially COMSOL software was selected for Modeling of Micro friction stir welding as multi physics phenomenon. Cad model of tool and plate was created by using its geometry features. Later modules of solid mechanics and heat transfer were also considered to analyze temperature and stress distribution for Aluminum plates. Usually in FSW, tool is moving along plate; to exhibit movement of tool in COMSOL, moving coordinate system was used which is plunged along tool axis otherwise it will complicate the problem. Geometry of model is uniform throughout thus only modeling of one plate is considered adequate in this software. Due to limitation of COMSOL in this particular phenomenon, it was replaced by ABAQUS Explicit. Thus for this study, it is significant to show movement of tool as weld strength is also affected by probe shape. Moreover for both similar and dissimilar materials it is necessary to model both plates which are difficult to exhibit on COMSOL. Also it is comparatively easy to analyze the variation in process parameters and material distribution using ABAQUS. Also this study has been divided into two steps, at first thin sheets are used for similar materials and thick sheets for dissimilar material which seems hard to model in COMSOL.

3.2.1 Introduction to ABAQUS

Depending upon our problem statement ABAQUS was considered for modeling of Friction stir welding. As movement of tool can be easily shown, also full plate geometry can be created easily. Thus modeling of Friction Stir Welding is well defined approach as it helps to reduce number of experimental trials by providing accurate result. As it has capability to deal with large complex problems and deformations. Different types of analysis can be easily performed in ABAQUS. Two types of analysis are done in ABAQUS which are ABAQUS Standard and ABAQUS explicit which act as analysis tools for different processes. ABAQUS Explicit was chosen as it provides finite strain, large displacement and large rotation formulation. ABAQUS Explicit deals with wide range of issues i.e. high speed deformation, coupled temp displacement etc. ABAQUS Explicit is usually act as best source for three dimensional model that contains

one or more of discontinuities i.e. buckling or local wrinkling of material or material degradation. It is used when models contains dynamic explicity as procedure type.[3]

A model was created in which a moving tool is moving along stationary plate. Dimensions of model were obtained from previous study. Thin plates of AL-5052 are used with dimensions of 100*65*1.20 mm. Three different shapes of probes were created i.e. circle, square and triangle. as shown in Figure 3.1.

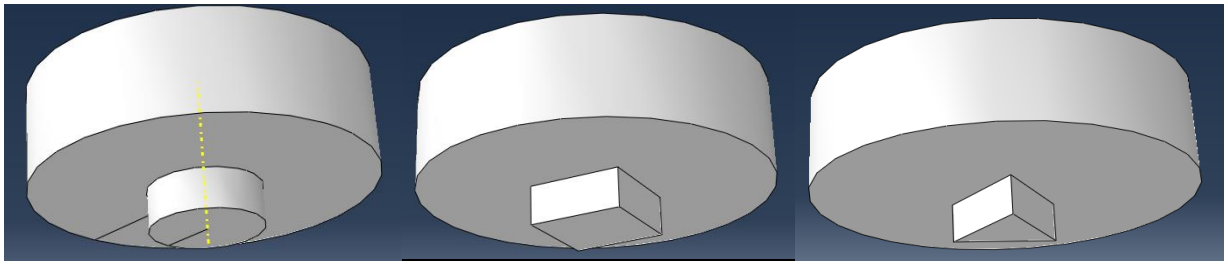

Figure 3.1 Three types of pin geometry

Material of tool is high speed steel; for circular tool, shoulder diameter is 7.5mm, pin diameter is 2.5mm and pin length is 0.85mm; for square and triangular tool length is 2mm. [20].

3.3 Modeling of similar materials

For modeling of tool and work piece, first geometry of plate is made and partition is done to show movement of tool in that particular field. After that tool geometry is created, for circular probe, shell revolution is chosen, while for square and triangular probe, solid extrusion is chosen as for AL plates. Assembly of plate and tool is illustrated in figure 3.2.

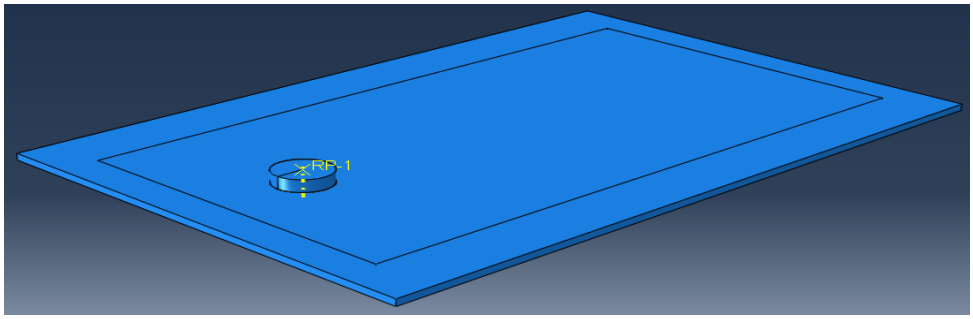

Figure 3.2. Cad model of similar materials in ABAQUS

3.3.1 Properties of Al-5052

For simulation, material properties are distributed into two stages i.e. thermo-physical and thermo-mechanical properties. Specific Heat, density and thermal conductivity are part of thermo-physical properties while thermo-mechanical consists of elasticity, plasticity and thermal expansion. In order to perform precise simulations, properties must be temperature dependent; poisson's ratio has constant value of 0.33, density 2.68E-09 (tonne/mm^3) and young's modulus of 703 MPa. Properties used for Al-5052 is mentioned in Table 3-2 [21]

Table 3-2 Temperature dependent properties of Al-5052

Temperature (^oC)	24	25	149	260	371
Thermal conductivity (mW/mm^o-C^o)	138	150	162	200	220
Thermal Expansion (C^o(1/K))	2.21E-05	2.28E-05	2.38E-05	2.48E-05	2.57E-05
Specific heat (mJ/mm^o-C^o)	8.80E+08	9.00E+08	1.00E+09	1.13E+09	1.20E+09

Value of plasticity is also temperature dependent and is exhibited in Table 3-3 [22]

Table 3-3. Temperature dependent rates of Yield stress, and Plastic Strain of Al-5052.

Yield Stress (MPa)	**Plastic Strain**	**Temperature (C^o)**
1.55E+02	0.00E+00	25
1.99E+02	1.51E-02	25
2.23E+02	4.27E-02	25
2.39E+02	7.24E-02	25
2.48E+02	9.35E-02	25
1.58E+02	0.00E+00	75

1.97E+02	1.89E-02	75
2.14E+02	4.65E-02	75
2.25E+02	7.57E-02	75
2.32E+02	9.62E-02	75
1.60E+02	0.00E+00	100
1.94E+02	2.27E-02	100
2.08E+02	4.97E-02	100
2.17E+02	8.00E-02	100
2.21E+02	9.84E-02	100
1.50E+02	0.00E+00	150
1.77E+02	2.76E-02	150
1.84E+02	5.57E-02	150
1.90E+02	8.49E-02	150
1.92E+02	9.89E-02	150
1.28E+02	0.00E+00	200
1.47E+02	3.46E-02	200
1.49E+02	5.24E-02	200
1.51E+02	7.14E-02	200
1.54E+02	9.78E-02	200

3.4 Modeling of Dissimilar Material

For modeling of two dissimilar materials, AA-6061-T651 and AA-5083-H-321 were considered. In this case thickness of sheets is larger than the previous discussed data. Dimensions of plates were 150*75*6.2 mm. Shoulder and pin diameter 22mm and 6mm respectively, pin length of 5.9mm, shoulder type chosen was concave as shown in figure 3.3. Previously effect of different variables on Friction stir welding of dissimilar materials was studied. Three different shapes of probe i.e. square, pentagon and hexagon, traverse speed of 10mm/min. 20mm/min and 30mm/min and rotational speed of 800rpm, 1000rpm and 1200rpm were considered. After analysis traverse speed of 10mm/min and 1000 rpm rotational speed and hexagonal shaped probed were found optimal as shown in figure 3.4.Result indicated that traverse speed was most influencing parameter as compare to other parameters. [23].

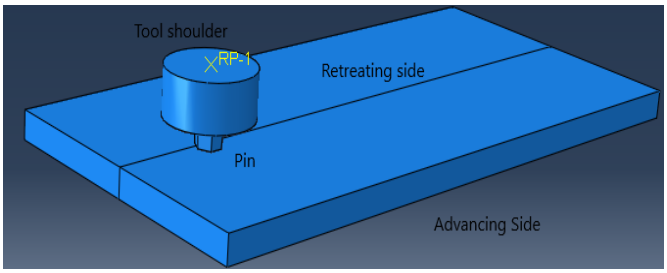

Figure 3.3: Cad model of dissimilar materials

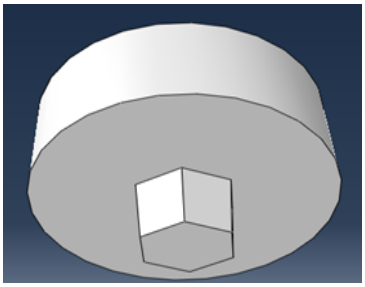

Figure 3.4. Cad model of hexagonal shaped probe

3.4.1 Properties of AA-6061-T651

For simulation, thermo mechanical and thermo physical properties of AA-6061 were chosen. It has some constant properties; density 2.70E-09 (tonne/mm^3), poisson's ratio 0.33 and Young's Modulus of 69300 MPa. Other premises are given in Table 3-4 [10].

Table 3-4 Temperature dependent properties of AA-6061

Temperature (^oC)	25	37.8	93.3	148.9	204.4	260	315.6	371.7	426.7
Thermal conductivity (mW/mm^o-C^o)	167	170	177	184	192	201	207	217	223
Thermal Expansion (C^o(1/K))	2.20E-05	2.35E-05	2.46E-05	2.57E-05	2.66E-05	2.76E-05	2.85E-05	2.96E-05	3.01E-05
Specific heat (mJ/mm^o-C^o)	8.96E+08	9.20E+08	9.78E+08	1.00E+09	1.03E+09	1.05E+09	1.07E+09	1.10E+09	1.13E+09

Values of yield stress and plastic strains are also dependent on temperature as illustrated in Table 3-5 [24]

Table 3-5. Temperature dependent values of Yield stress, and Plastic Strain of AA-6061.

Yield Stress (MPa)	**Plastic Strain**	**Temperature (C^0)**
1.39E+02	0.00E+00	20
1.42E+02	6.82E-02	20
1.46E+02	1.67E-01	20
1.49E+02	2.30E-01	20
1.53E+02	3.15E-01	20
1.05E+02	0.00E+00	150
1.10E+02	6.60E-02	150
1.12E+02	1.51E-01	150
1.17E+02	2.25E-01	150
1.18E+02	2.98E-01	150
8.15E+01	0.00E+00	250
8.29E+01	5.23E-02	250
8.57E+01	1.26E-01	250
8.71E+01	2.25E-01	250
8.99E+01	3.53E-01	250
3.10E+01	0.00E+00	350
3.10E+01	9.87E-02	350
1.00E+01	0.00E+00	450
1.14E+01	1.05E-01	450

3.4.2 Properties of AA-5083-H-321

Other material chosen for dissimilar Friction Stir Welding is AA-5083-H-321. It has constant value of density, poisson's ratio and Young's modulus i.e. 2.66E-09 (tonne/mm^3), 0.33 and 70300 MPa respectively. Table 3-6 and 3-7 exhibits other mechanical properties required for simulation [25] and [26].

Table 3-6 Temperature dependent properties of AA-5083

Temperature (^oC)	80	180	280	380	480	580
Thermal conductivity (mW/mm^o-C^o)	122.7	131.6	142.3	152.5	159.5	177.2
Thermal Expansion ($C^o(1/K)$)	2.21E-05	2.28E-05	2.38E-05	2.48E-05	2.57E-05	2.59E-09
Specific heat ($mJ/mm^{o-}C^o$)	9.84E+08	1.04E+09	1.08E+09	1.13E+09	1.18E+09	1.26E+09

Table 3-7. Temperature dependent values of yield stress, and plastic strain of AA-5083.

Yield Stress (MPa)	**Plastic Strain**	**Temperature (C^o)**
1.64E+02	0.00E+00	45
2.03E+02	1.77E-02	45
2.35E+02	3.19E-02	45
2.63E+02	5.67E-02	45
2.91E+02	7.80E-02	45
3.20E+02	1.06E-01	45
3.56E+02	1.81E-01	45
3.81E+02	2.77E-01	45
3.89E+02	3.37E-01	45
4.00E+02	3.87E-01	45
1.78E+02	0.00E+00	90
2.35E+02	2.13E-02	90
2.77E+02	3.90E-02	90
3.13E+02	6.74E-02	90
3.38E+02	9.57E-02	90
3.63E+02	1.42E-01	90
3.77E+02	1.81E-01	90
3.92E+02	2.34E-01	90
4.02E+02	2.70E-01	90

3.5 Model Meshing and Boundary Conditions:

3.5.1 Boundary Conditions

Simulations was divided into three steps; in step one tool is moved lower, while in step 2 tool is rotated, in step 3 tool is moved along plate at required distance. Procedure type for each step was defined as dynamic explicit. Different time increment is given for each steps depending upon the traverse speed. General contact interaction was added to define contact between all regions of a model with single interaction. Nine samples of experiments are shown in Table 3-8. [20]

Table 3-8 Simulation runs

Traverse speed (mm/min)	**Rotational speed (rpm)**	**Probe shape**
100	2000	circle
100	2500	triangle
100	3250	square
200	2000	triangle
200	2500	square
200	3250	circle
400	2000	square
400	2500	circle
400	3250	triangle

After adding step time, interaction properties are added, general contact is chosen, and constraints are applied on tool part as it is rigid part. Interaction property is applied for general contact. As all properties chosen are temperature dependent thus a predefined temperature is applied as for stress, displacement analysis it will provide thermal strain. Boundary conditions are applied for particular sample. Three boundary conditions were added;

1. Symmetry/Asymmetrical/ Encastre

Encastre was chosen for both similar and dissimilar plates : U1=U2=U3=UR1=UR2=UR3=0 thus remains constant.

2. Displacement/rotation

For step 1 where tool moves lower distance of 0.85mm for thin sheet and for thick sheet distance of 5.9mm was given. Also for step 3 tool moves along plate at distance of 5mm for both thin and thick sheets was given

3. Velocity and Angular rotation

In step 2 tool rotates along plate thus rotational speed relative to each sample was added in this boundary condition

3.5.2 Meshing Conditions:

Friction stir welding process is modeled in ABAQUS FEM code. Both work piece and tool were modeled. After application of boundaries conditions and other properties, meshing was done. In many nonlinear solutions the material in the structure or process deals with large deformations. Thus due to this mesh is unable to perform required results or analysis may terminate because of numerical reasons. Adaptive meshing technique was adopted to periodically minimize the distortion in the mesh. For this purpose Pure Lagrangian model was selected as mesh moves with the material. With this approach it is easy to apply boundary conditions. In Lagrangian adaptive mesh domains, the mesh will follow the material in direction normal to the boundary. Nodes are free to adapt within and along the edges of the region but cannot leave it. [3] Both tool and work piece were meshed by applying seed on parts and edges respectively. The tool was meshed by applying seeds and divided into 189 elements and consists of 193 nodes. For plate first elements type was choses and divided into 17796 elements and consists of 22490 nodes. But before that it is necessary to define element type, explicit; Coupled temperature displacement was chosen. It is used for thermo mechanical processes which does not involve large deformations or where stress analysis is dependent on temperature .

For circular tool, part type chosen was discrete rigid thus it can be easily meshed by applying seeds, while for square and triangle tool tet shaped element type was assigned.

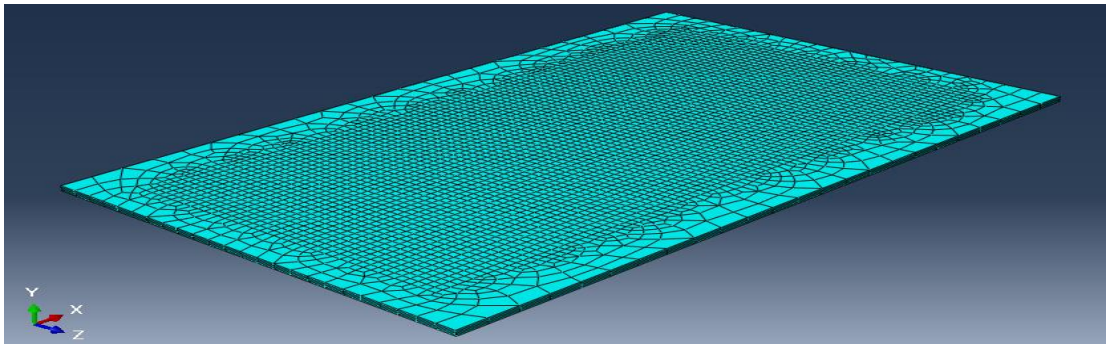

Figure 3.5. Meshing of AL plate

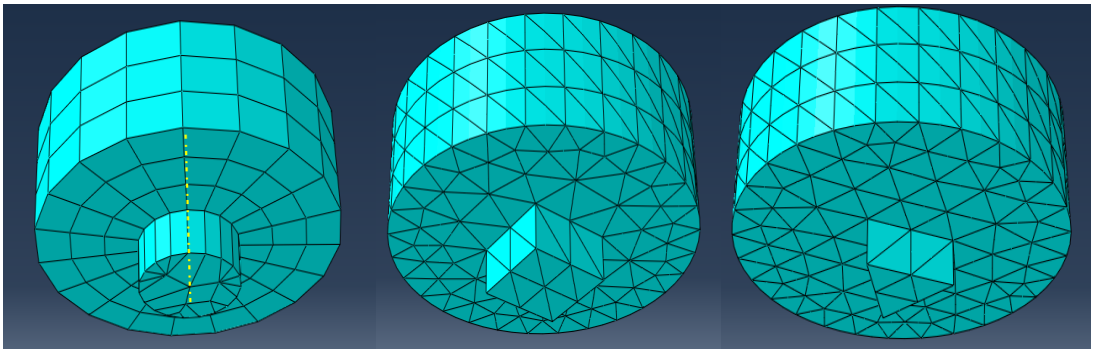

Figure 3.6. Meshing of tool

3.6 Modeling of Tensile Specimen:

To evaluate ultimate tensile strength for each sample of similar and dissimilar materials, it is necessary to calculate stress strain curve. For this purpose, tensile specimen was modeled using ABAQUS. This model will incorporate residual stresses obtained from plate model as input and then will provide stress strain curve for each samples. Thus nine tensile specimen models were created for nine similar materials sample and one for dissimilar plates. Both of the previous studies considered tensile specimen on the basis of ASTM E8/ E8M to obtain ultimate tensile strength. Thus standard sample size was modeled using ABAQUS as shown in figure 3.7. Properties were obtained from plate model to assign tensile sample such as young's modulus, poisson's ratio, yield stress and plastic strain. Coupling constraint was applied to one side of the plate and bottom of the plate was made fixed. Displacement was given to obtain particular stresses on the middle of the plate. After that two boundary conditions were added.

- Encastre: U1=U2=U3=UR1=UR2=UR3=0 fixed at one end

- Displacement and rotation

Two predefined field was considered; one residual stresses and other was temperature. To determine required tensile strength, average value of residual stresses was added in residual stress predefined field as input for each sample.

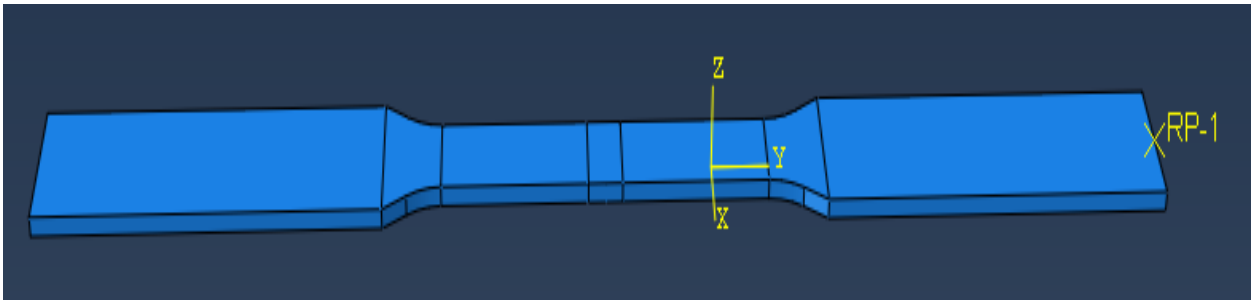

Figure 3.7. Model of Tensile specimen for similar materials.

Residual stresses from plate model were incorporated choosing Predefined field type stress. Meshing was obtained by applying seeds along edges; fine meshing is done around middle portion of plate. The specimen was divided by 4160 elements and 5995 nodes, as shown in figure 3.8.

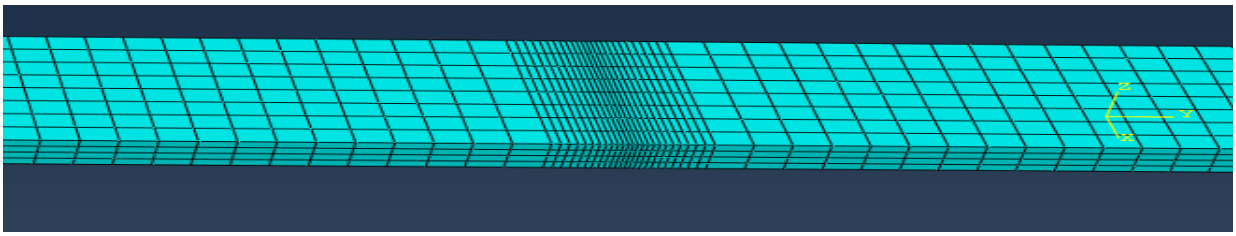

Figure 3.8. Meshing of tensile sample

CHAPTER 4: RESULTS & DISCUSSIONS

This chapter will illustrate results obtained from modeling of plates and tensile specimen. Also different graphs obtained from results will be discussed and verified order to compare previous experimental results.

4.1 For Similar Materials

4.1.1 Model # 1

Nine samples were modeled using ABAQUS, and residual stresses obtained from plate model were incorporated in tensile specimen model. Below Figure 4.1 exhibits results obtained from Sample 1 i.e. probe circular, rotational speed of 2000 rpm, traverse speed of 100mm/min.

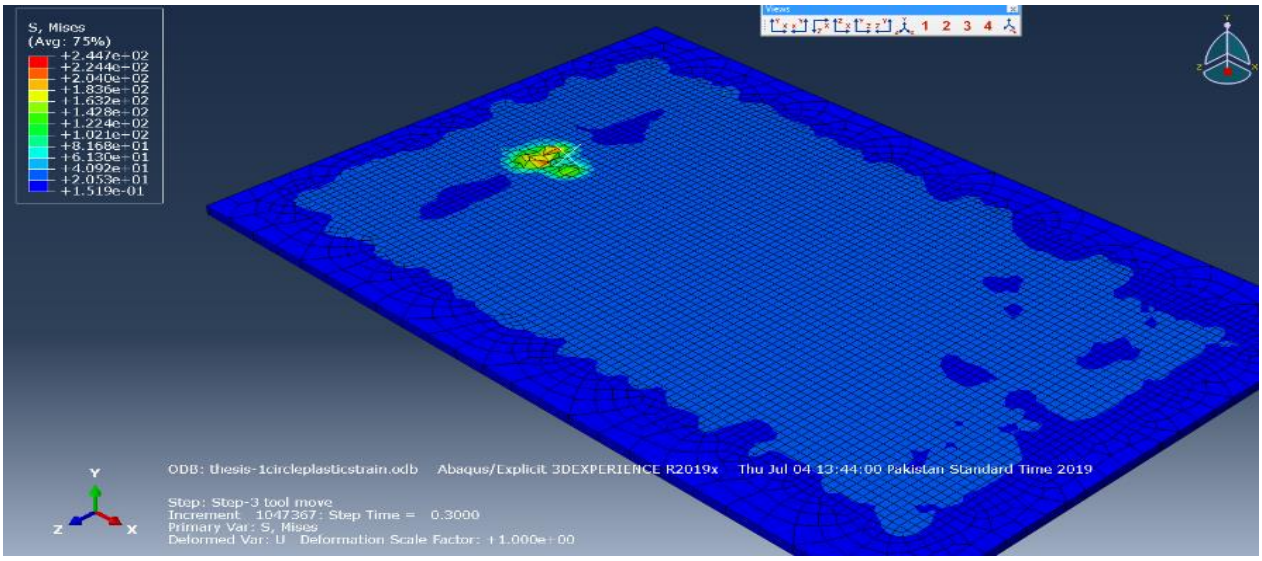

Figure 4.1. Three dimensional Residual stresses obtained from plate model (circular probe, ν=100 mm/min, ω=2000 rpm)

These results obtained from plate model describes that residual stresses occurs when expansion and contraction of material takes place during welding. Value of residual stresses appears to be maximum when tool contacts with plate and when it rotates thermal stresses are induced. Their effect is significant i.e. 244MPa when tool moves along plate at particular distance calculated i.e. 5mm.

Plate model results were further added as input in tensile specimen model. Hence modeling of tensile specimen for each sample is similar; only change that occurred was in the values of initial stresses obtained from plate model. From the results obtained from tensile specimen, stress strain

values were predicted and a curve was generated in order to verify previous resulted graphs. Figure 4.2 shows the tensile specimen results obtained for sample 1.

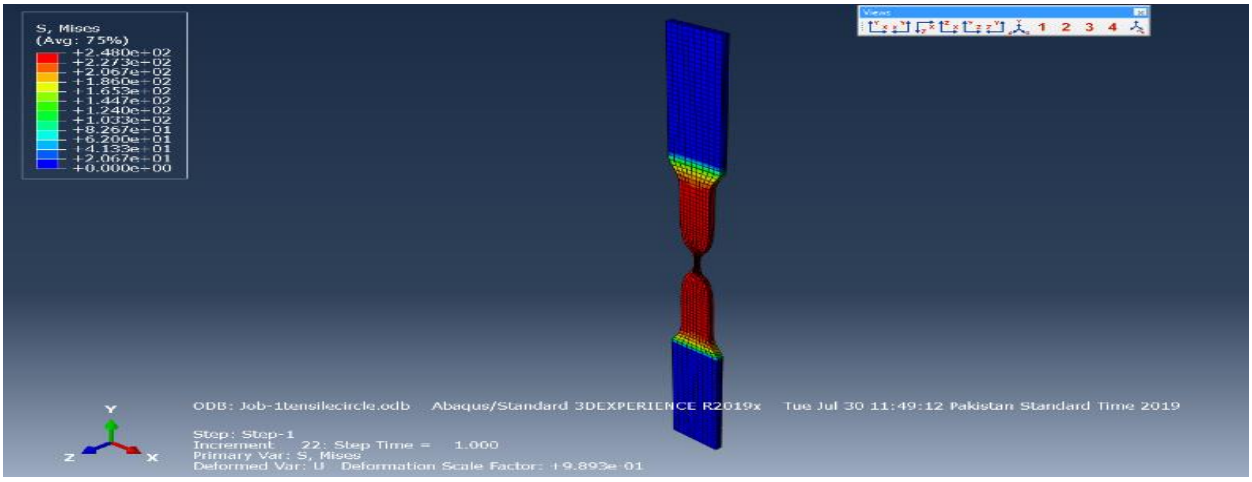

Figure 4.2. Predicted stresses obtained from tensile specimen model for sample 1(circular probe, ν=100 mm/min, ω=2000 rpm)

4.1.2 Model # 2

Next model was run for triangular probe with traverse speed of 100mm/min and rotational speed of 2500 rpm. Residual stresses were found when plate and tool interconnects due to material distribution. Thus it can be seen that welding phenomenon is highly dependent on theses process parameters, also welding quality can be improved using such parameters.

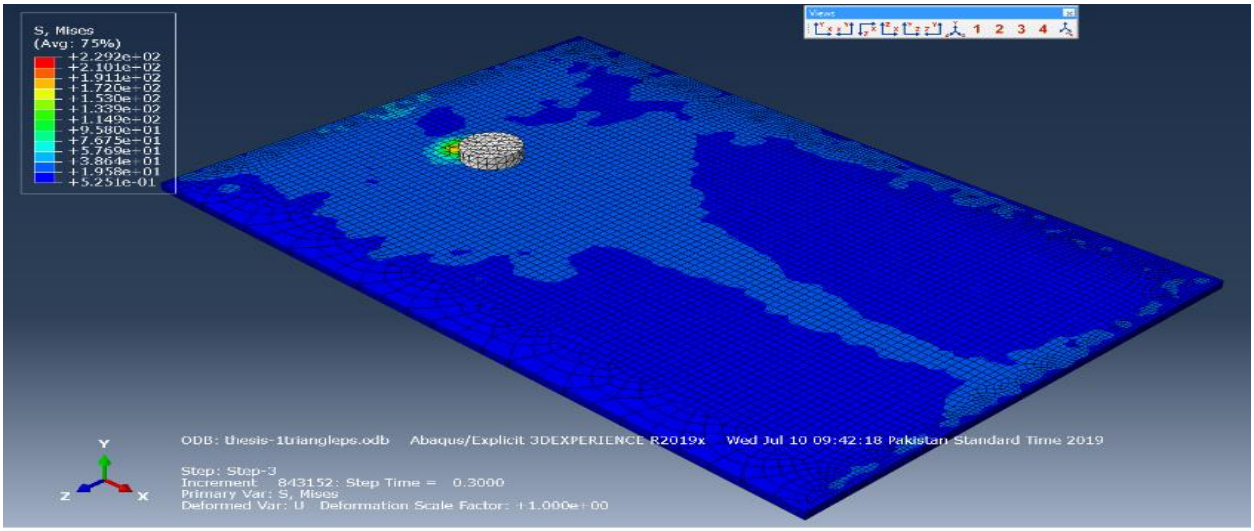

Figure 4.3. Three dimensional Residual stresses obtained from plate model (Triangular probe, ν=100 mm/min, ω=2500 rpm)

4.1.3 Model # 3

Further similar model was analyzed for square tool probe at traverse speed of 100mm/min and rotational speed of 3250rpm. Below figure 4.4 shows the residual stresses obtained during simulation of this model.

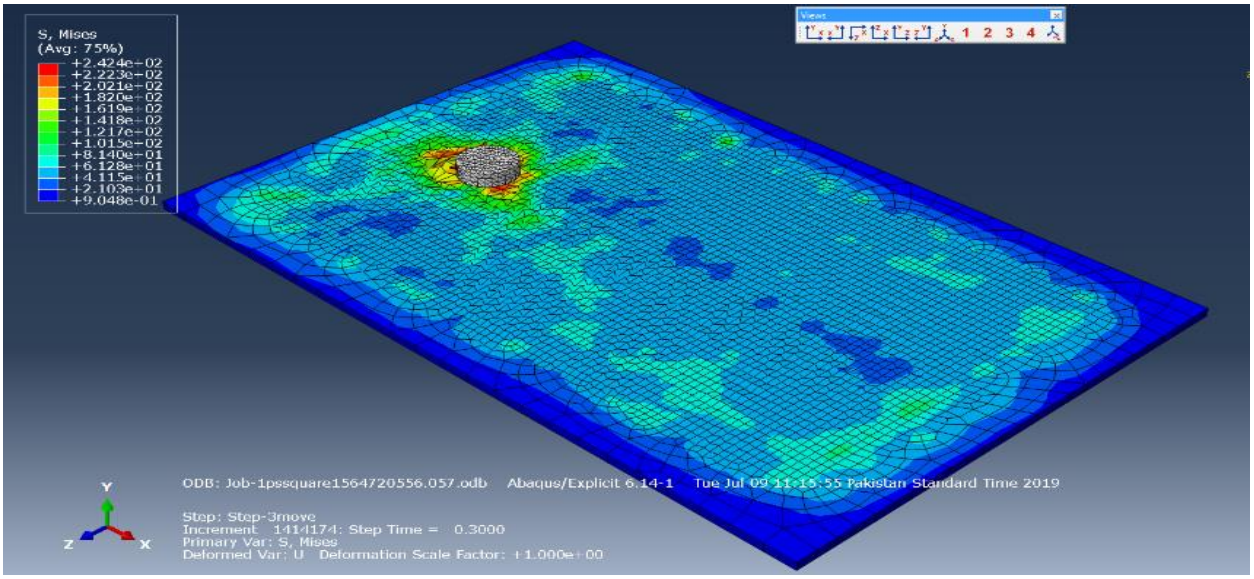

Figure 4.4. Three dimensional Residual stresses obtained from plate model (Square probe, ν=100 mm/min, ω=3250 rpm)

4.1.4 Comparison of samples obtained at traverse speed of 100mm/min

The results obtained from above mentioned models were incorporated in their tensile model to analyze stress strain curve. A graph was generated to compare their results on stress strain values.

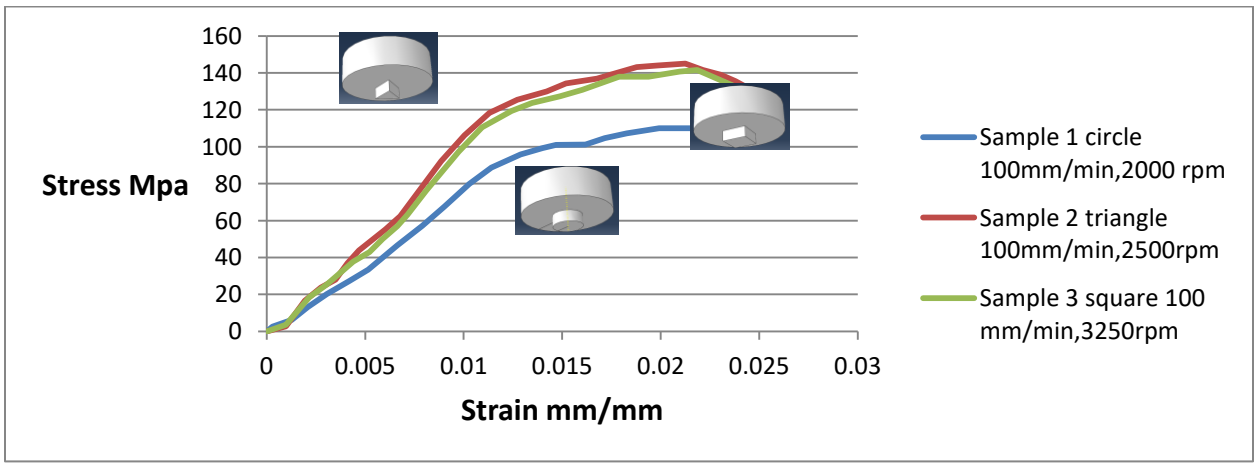

Figure 4.5. Comparison of stress strain values of three samples at constant traverse speed 100mm/min

4.1.5 Model #4

Below figure shows residual stresses obtained from sample 4, triangular probe running at traverse speed of 200mm/min and rotational speed of 2000 rpm. Next three models were simulated at traverse speed 200mm/min

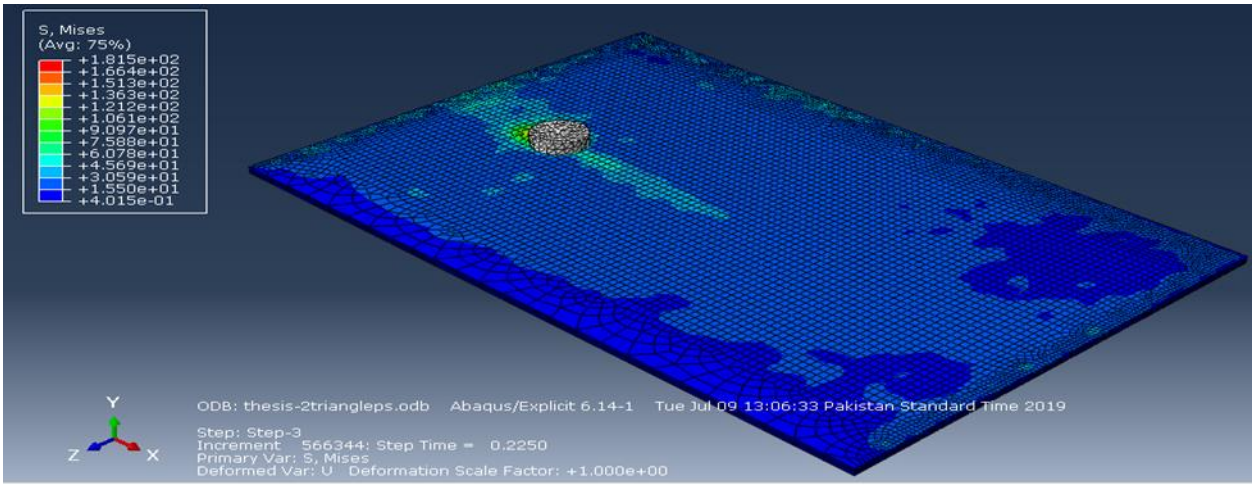

Figure 4.6. Three dimensional Residual stresses obtained from plate model (Triangular probe, v=200 mm/min, ω=2000 rpm)

4.1.6 Model # 5

Residual stresses generated at rotational speed of 2500rpm, traverse speed of 200mm/min for square probe shape can be seen in the figure 4.7 below

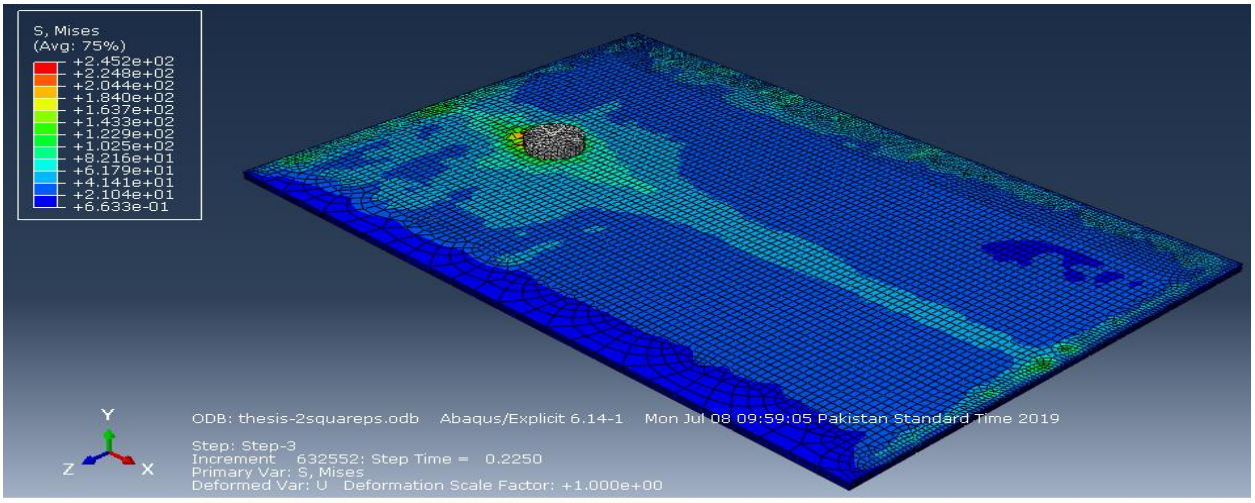

Figure 4.7. Three dimensional Residual stresses obtained from plate model (square probe, v=200 mm/min, ω=2500 rpm)

4.1.7 Model # 6

Result of residual stresses for circular probe at constant traverse speed i.e. 100mm/min and rotational speed of 3250 rpm is shown in figure 4.8.

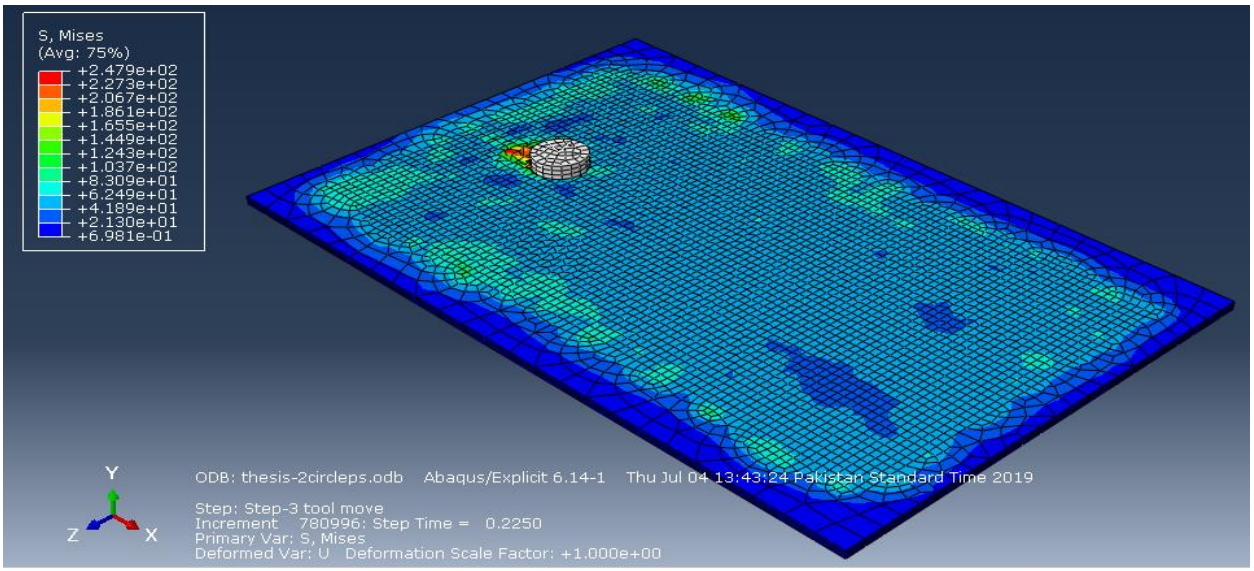

Figure 4.8. Three dimensional Residual stresses obtained from plate model (circular probe, ν=200 mm/min, ω=3250 rpm)

4.1.8 Comparison of samples obtained at traverse speed of 200mm/min

The results obtained from above mentioned models were incorporated in their tensile model to analyze stress strain curve.

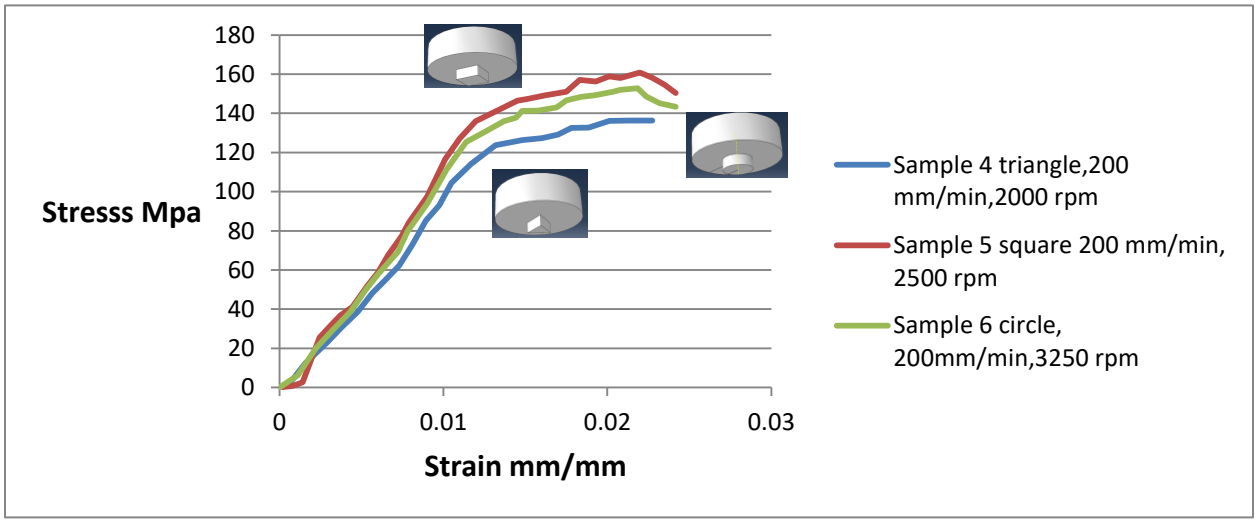

Figure 4.9. Comparison of stress strain values of three samples at constant traverse speed 200mm/min

4.1.9 Model # 7

Below figure 4.10 illustrates the residual stresses obtained for square probe at traverse speed of 400mm/min and rotational speed of 2000 rpm.

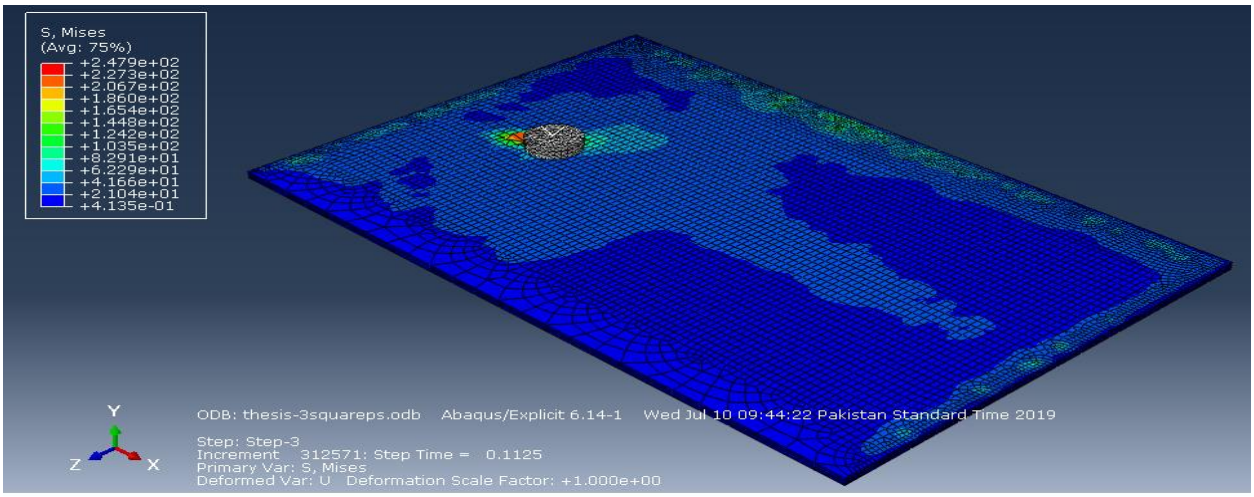

Figure 4.10. Three dimensional Residual stresses obtained from plate model (square probe, v=400 mm/min, ω=2000 rpm)

4.1.10 Model # 8

Effect of residual stress obtained from below model seems maximum when tool starts moving along the plate as seen in figure 4.11.

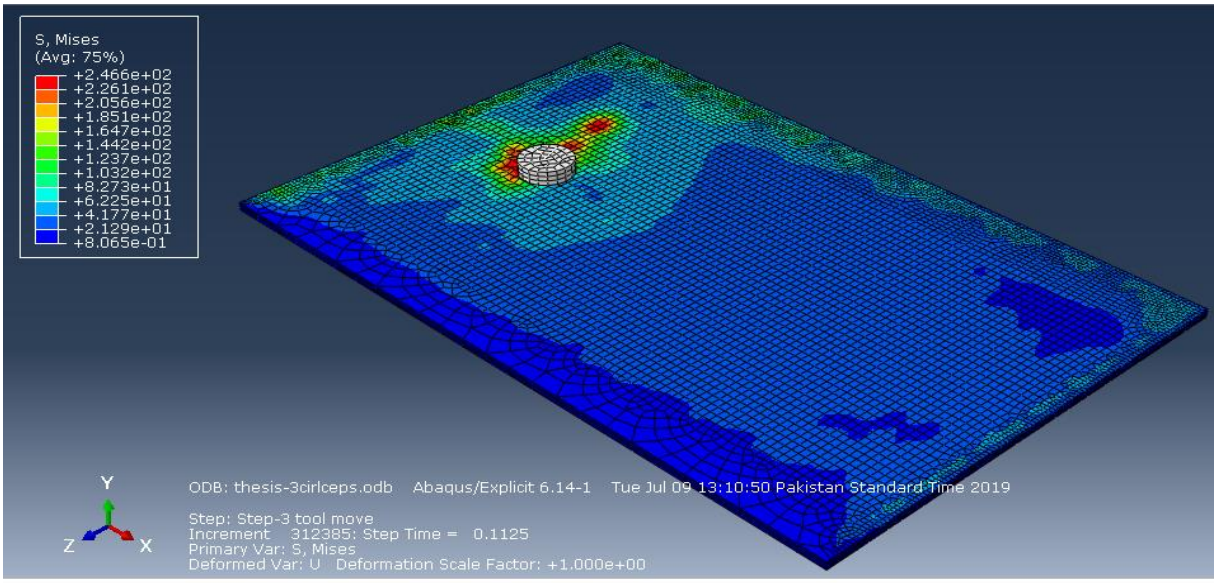

Figure 4.11. Three dimensional Residual stresses obtained from plate model (Circular probe, v=400 mm/min, ω=2500 rpm)

4.1.11 Model # 9

Last model for similar materials was obtained for triangular probe. After running the job, results were analyzed to observe the behavior of tool and plate with materials distribution. Thus residual stresses were studied at traverse speed of 400mm/min and rotational speed of 3250 rpm which can be seen from below figure 4.12.

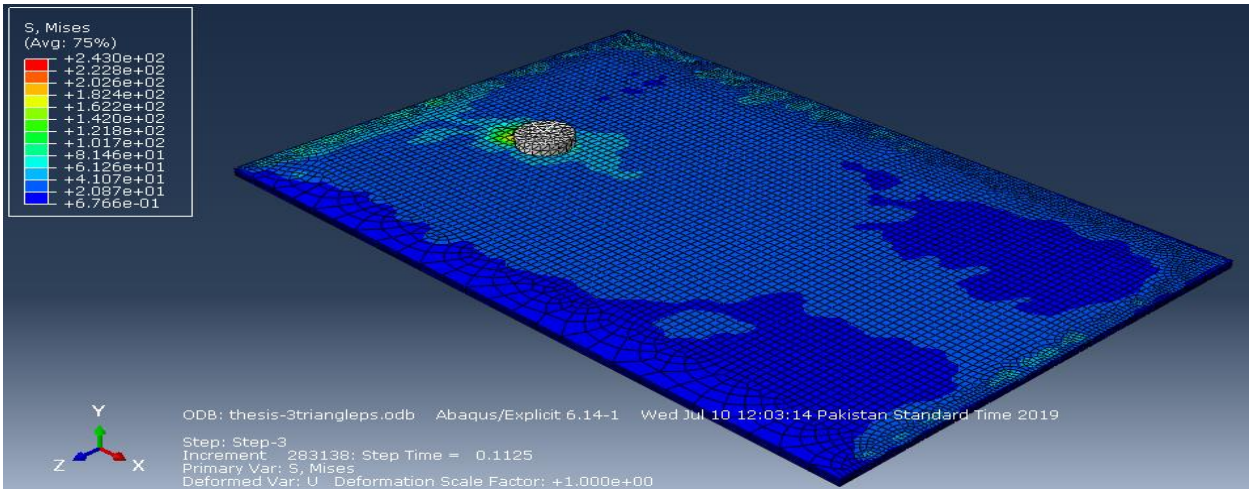

Figure 4.12. Three dimensional Residual stresses obtained from plate model (Triangular probe, v=400 mm/min, ω=3250 rpm)

4.1.12 Comparison of samples obtained at traverse speed of 400mm/min

The results obtained from above mentioned models were incorporated in their tensile model to analyze stress strain curve.

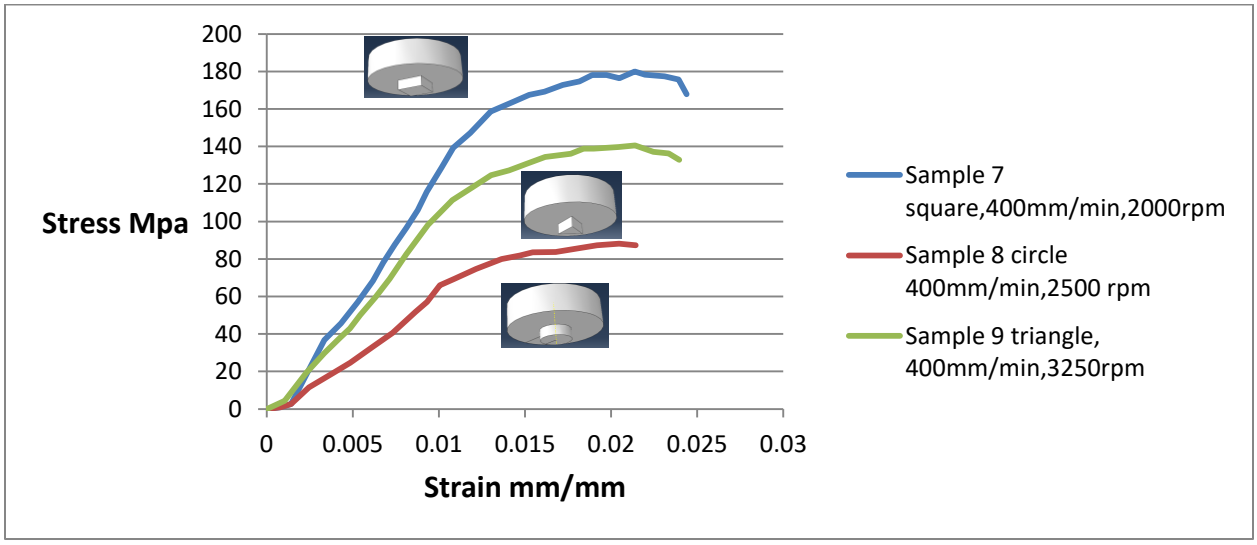

Figure 4.13 Comparison of stress strain values of three samples at constant traverse speed 400mm/min

4.1.13 Effect of different probe shapes on welding:

After obtaining and simulating models, results were compared on the basis of tool shapes and their effect of stress strain curve was studied. Figures below show behavior of tool shape, traverse speed and rotational speed on stress strain curve.

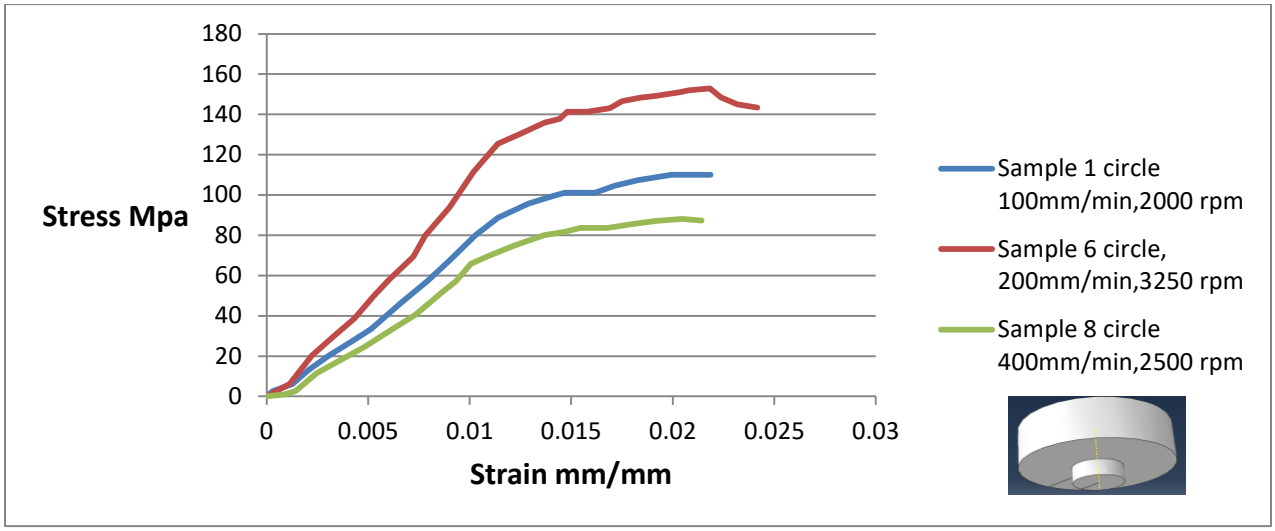

Figure 4.14 Comparison of stress strain values of three samples for circular probe.

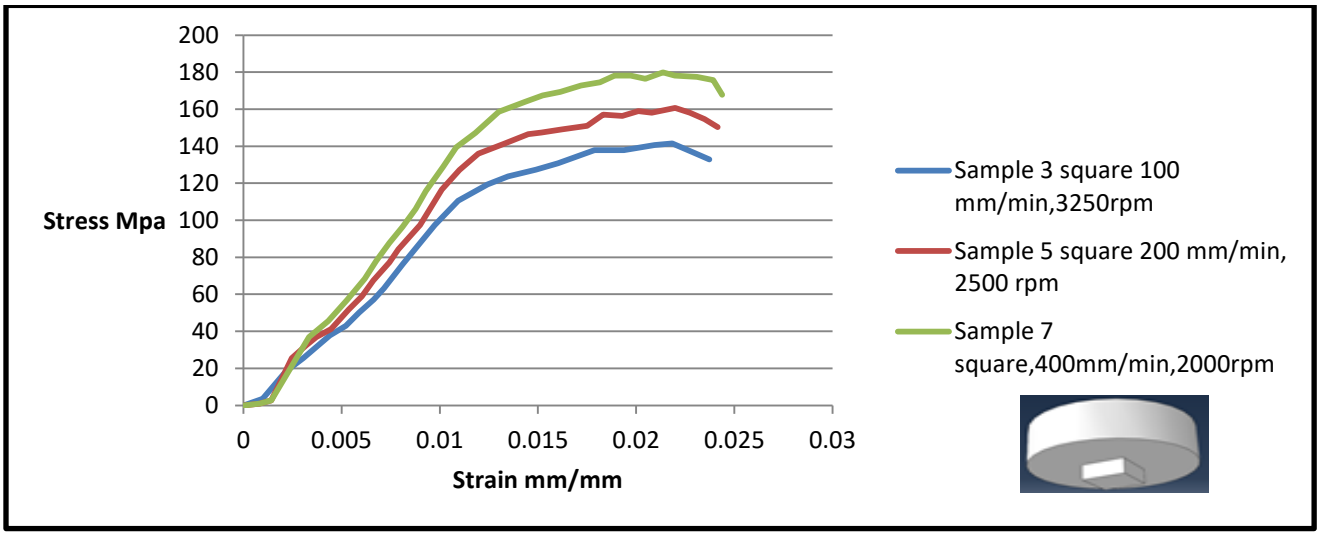

Figure 4.15 Comparison of stress strain values of three samples for square probe.

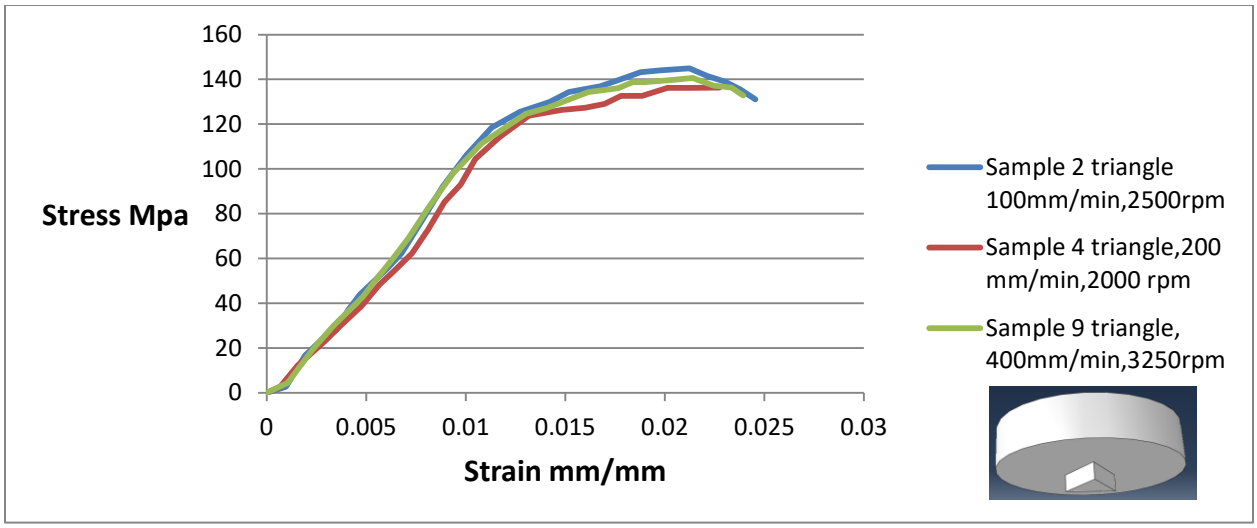

Figure 4.16 Comparison of stress strain values of three samples for triangular probe.

4.1.14. Comparison of rotational speed at 2000rpm, 2500 rpm and 3250rpm

All the samples were compared on the basis of rotational speed, in order to observe the influence of each parameter during FSW. From graphs it can be concluded that greater the rotational speed more will be tensile strength as 3250 rpm was considered as optimal.

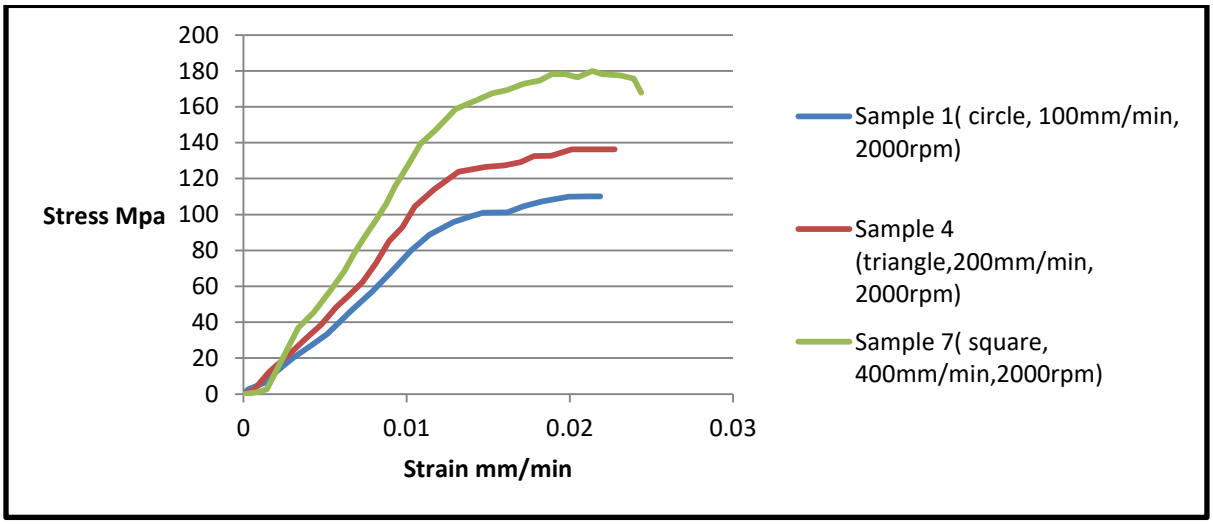

Figure 4.17 Comparison of stress strain values of samples at 2000rpm.

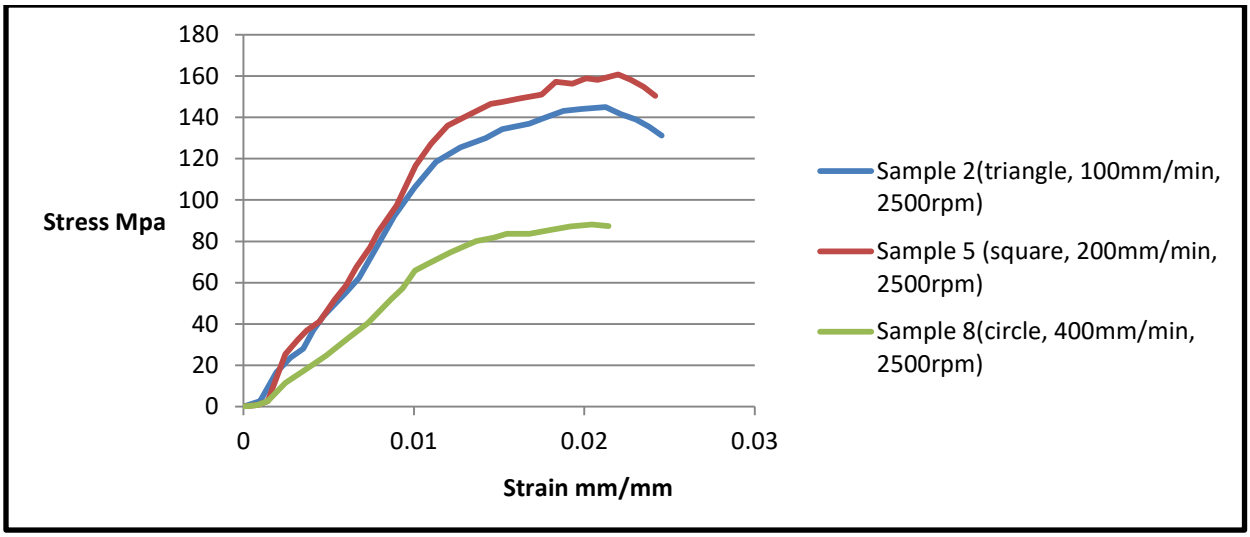

Figure 4.18 Comparison of stress strain values of samples at 2500rpm.

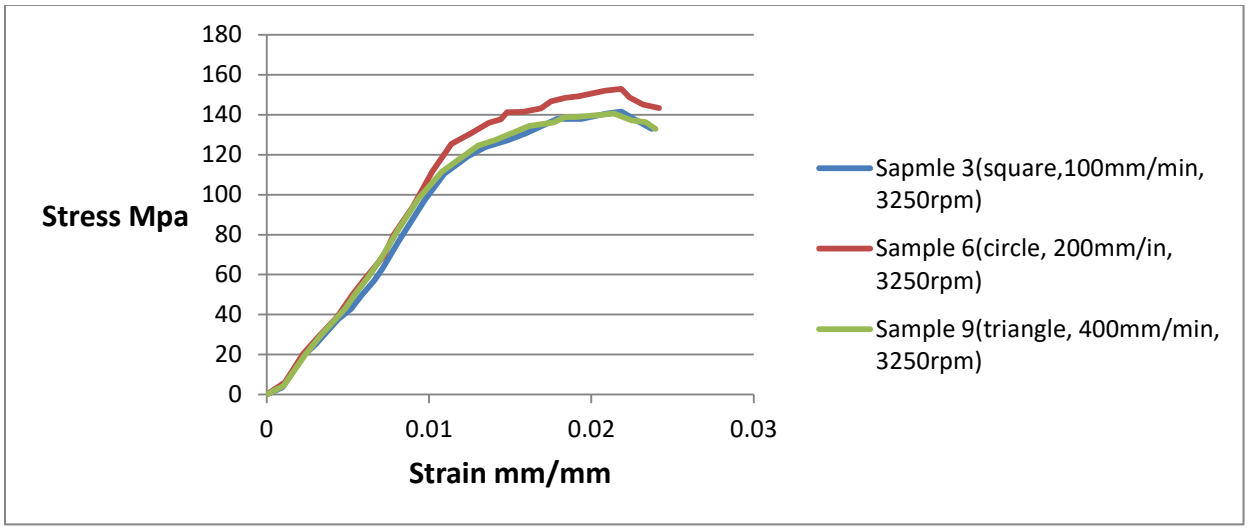

Figure 4.19 Comparison of stress strain values of samples at 3250rpm.

4.2 Results obtained from similar materials:

All these results obtained from above analysis were arranged graphically to illustrate their effect on stress strain curve.

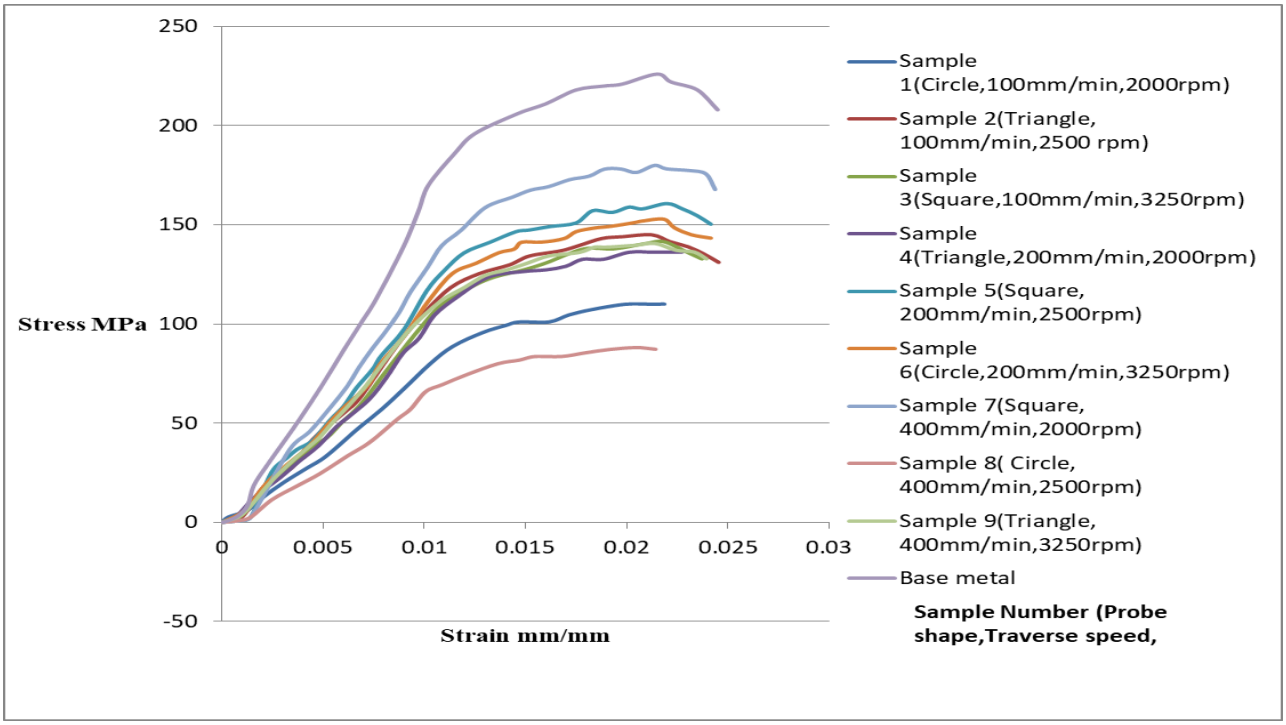

Figure 4.20 Stress strain curve for similar materials.

Ultimate tensile strength was evaluated from this stress strain curve which is exhibited in the Table 4-1.

Table 4.1 shows ultimate tensile strength for each sample

Sample #	Probe Shape	Rotational Speed (RPM)	Traverse Speed (mm/min)	Ultimate Tensile Strength Obtained from experimental data	Ultimate Tensile Strength (Simulation results)	Percentage difference
1	circle	2000	100	108	101	**5.71%**
2	triangle	2500	100	143	143	
3	square	3250	100	140	137	**2.1%**
4	triangle	2000	200	140	132	**5.88%**
5	square	2500	200	160	156	**2.5%**
6	circle	3250	200	150	147	**2.46%**
7	square	2000	400	180	178	**1.11%**
8	circle	2500	400	88	81	**8.28%**
9	triangle	3250	400	141	137	**2.8%**

Above table 4.1 presents the ultimate tensile strength obtained after simulating experimental data and ultimate tensile strength obtained from previous study. Thus minimal difference can be seen in both values which can be negligible. These experimental results were analyzed using ANOVA analysis in the past, which concluded optimal values of parameters suitable for particular material type and thickness. Thus a confirmation run was conducted to observe the behavior of these optimal values i.e. 200mm/min traverse speed and 3250 rpm rotational speed for a square probe and its effect on stress strain values was observed. Figure 4.18 shows stress analysis obtained from optimal parameters.

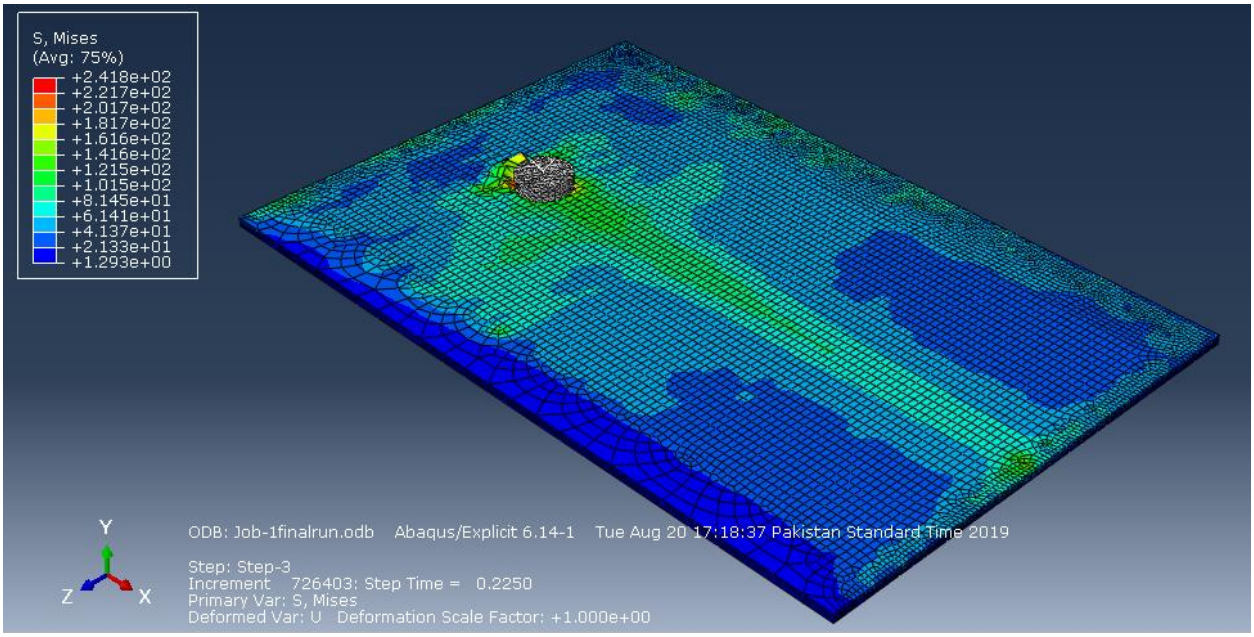

Figure 4.21 Three dimensional Residual stresses obtained from plate model (Square probe, v=200 mm/min, ω=3250 rpm)

These residual stresses obtained from above model were added as initial values for tensile model to obtain stress strain values.

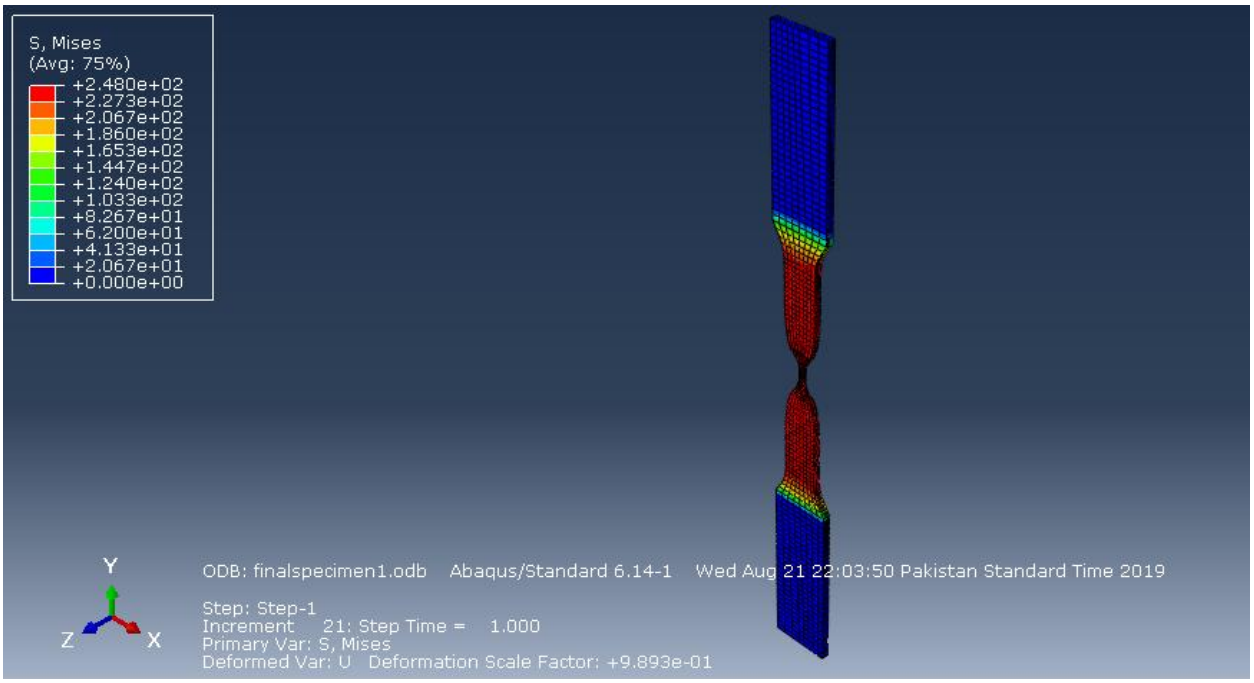

Figure 4.22 Predicted stresses obtained from tensile specimen model (square probe, ν=200 mm/min, ω=3250 rpm)

Taking account tensile model, graph was plotted to evaluate stress strain curve. Thus ultimate tensile strength obtained was 183MPa which shows these parameters are optimal for FSW of Al-5052. Also this value has validated ultimate tensile strength obtained experimentally.

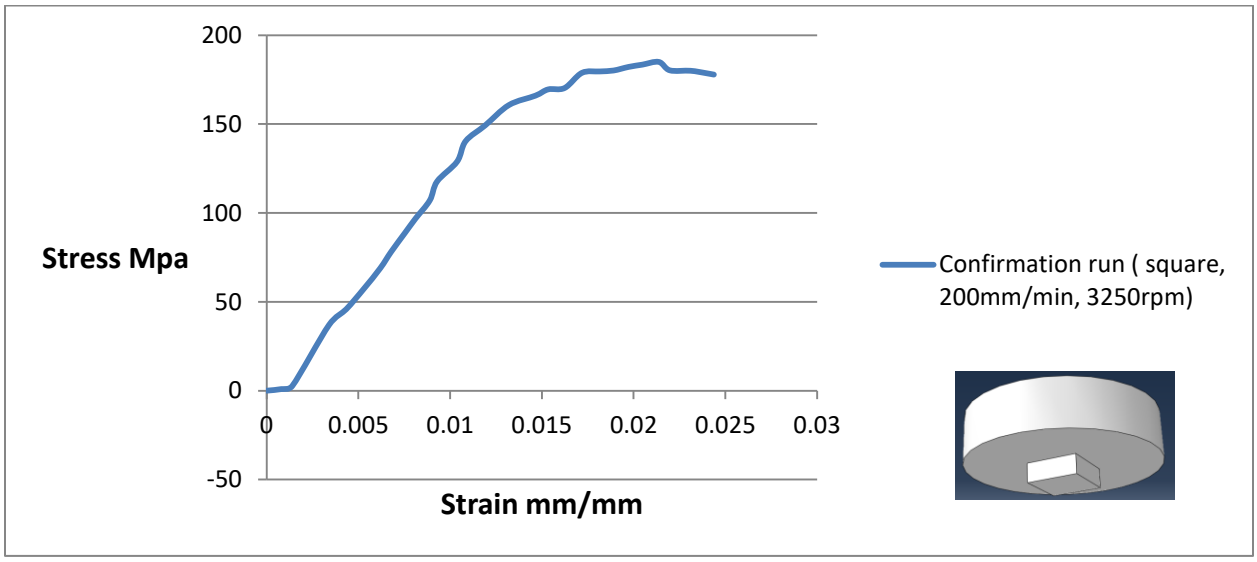

Figure 4.23 Stress strain curve obtained by plotting results of optimal parameters (square probe, 200mm/min traverse speed and 3250 rpm rotational speed)

4.3 For Dissimilar Materials:

Model of dissimilar materials was also simulated to observe the effect of residual stresses on both plates when tool moves along them. Tool moves along the plate for 5 mm, as a result stresses were produced and their effect was significant at this point. Figure 4.21 below exhibits the behavior of residual stresses on plates as a result of expansion and contraction occurred during material deformation.

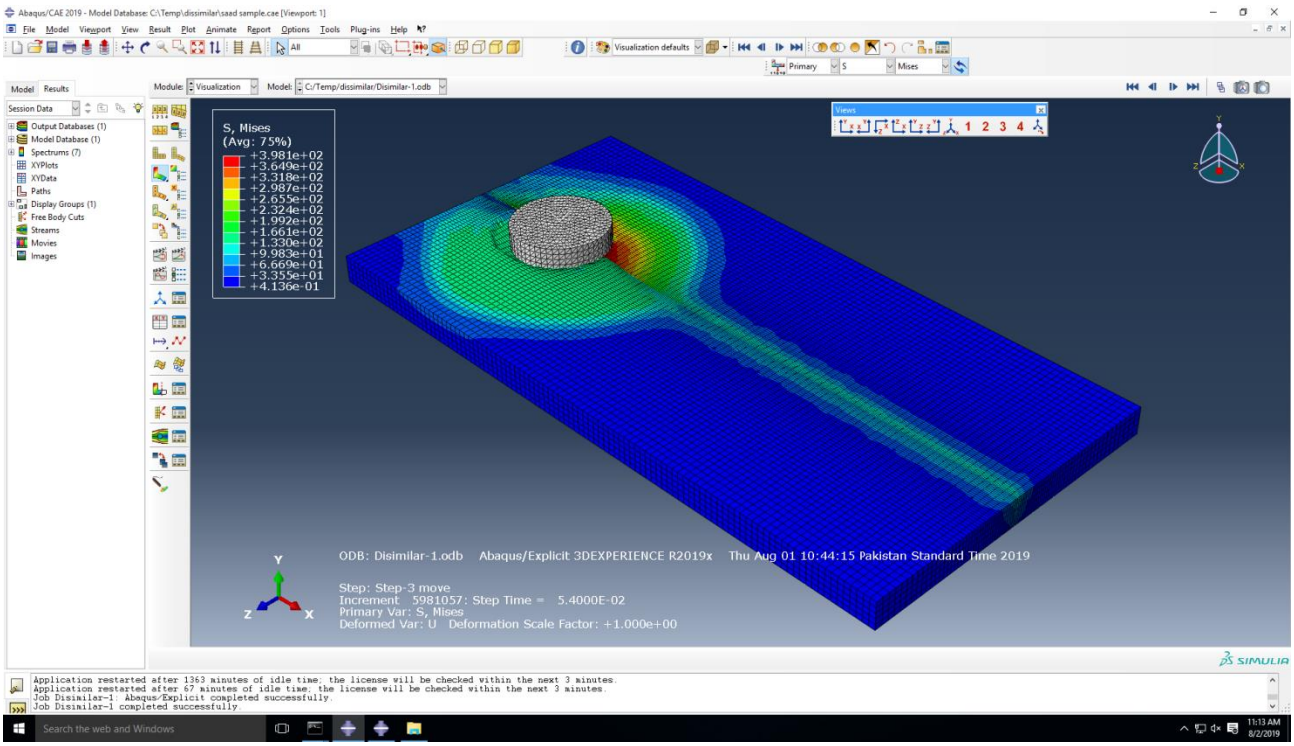

Figure 4.24 Residual stresses obtained for dissimilar materials with hexagonal probe shape, traverse speed 10mm/min and rotational speed of 100rpm.

These stresses were added as input in tensile model to calculate stress strain values for ultimate tensile strength. Below figures show the results obtained during simulation of tensile specimen.

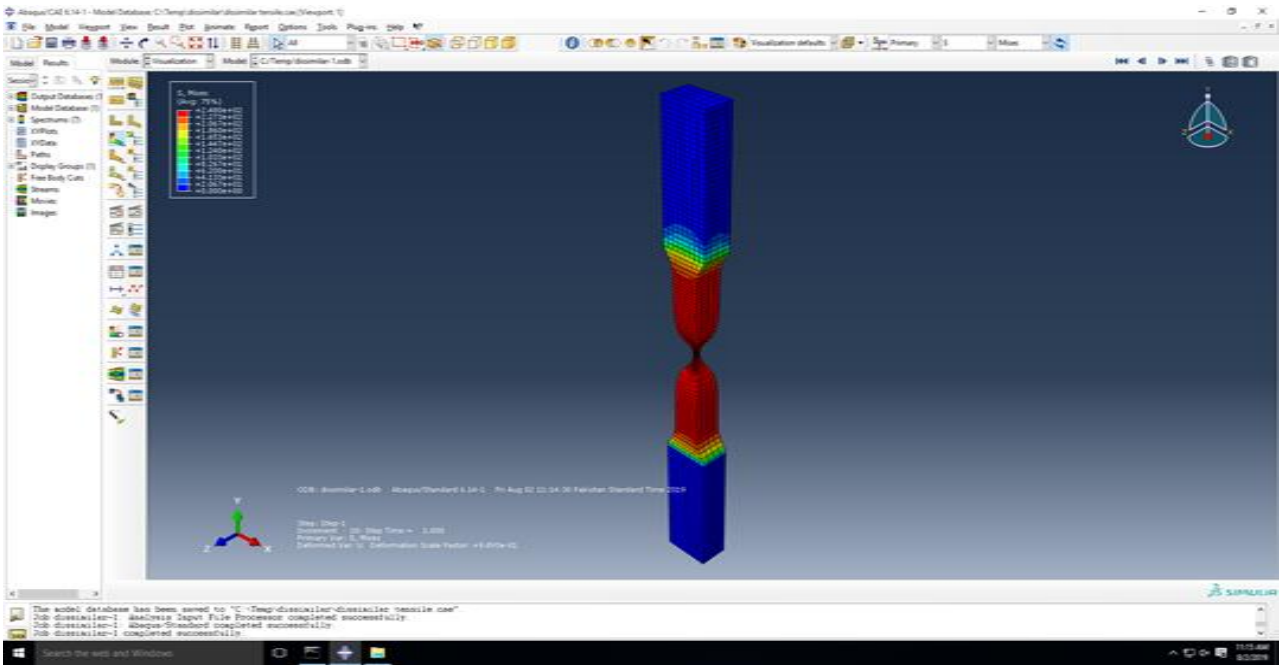

Figure 4.25 Tensile model for dissimilar materials; Aluminum AA5083 and AA6061

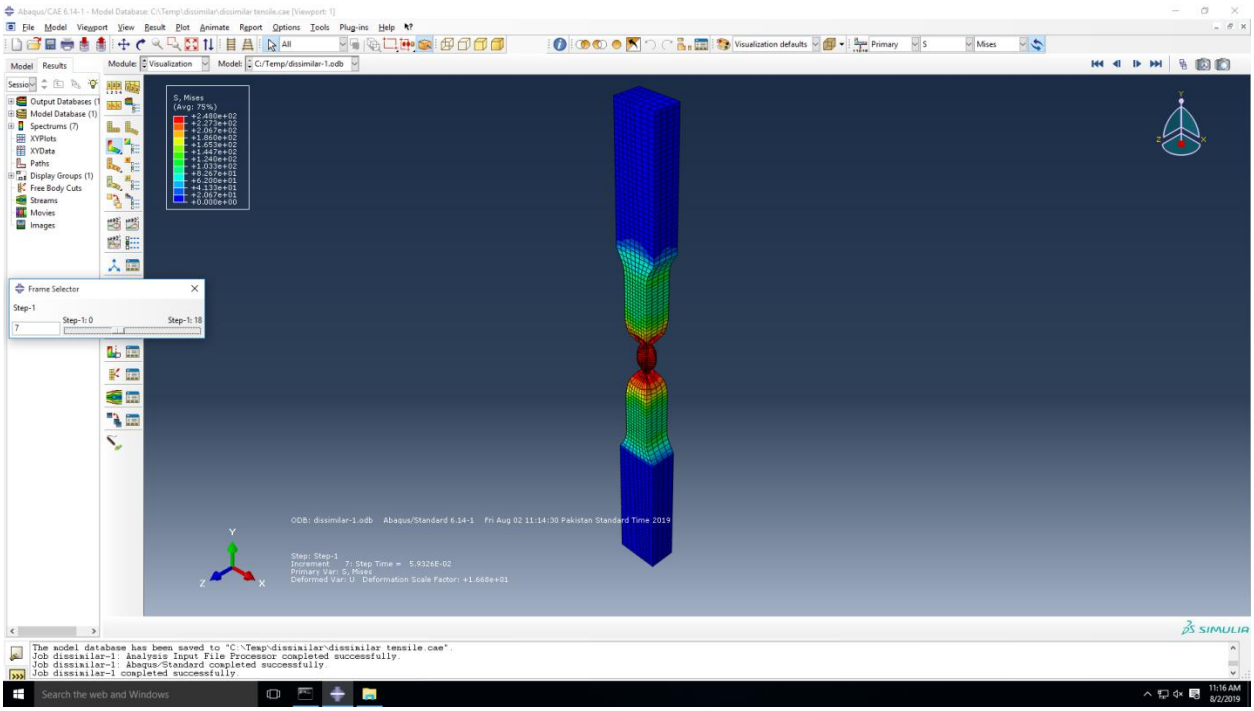

Figure 4.26 Residual stresses obtained for Aluminum AA5083 and AA6061

These results were further represented in graph to show their stress strain curve, ultimate tensile strength was found to be 202 Mpa for this sample which seems having good welding quality for FSW.

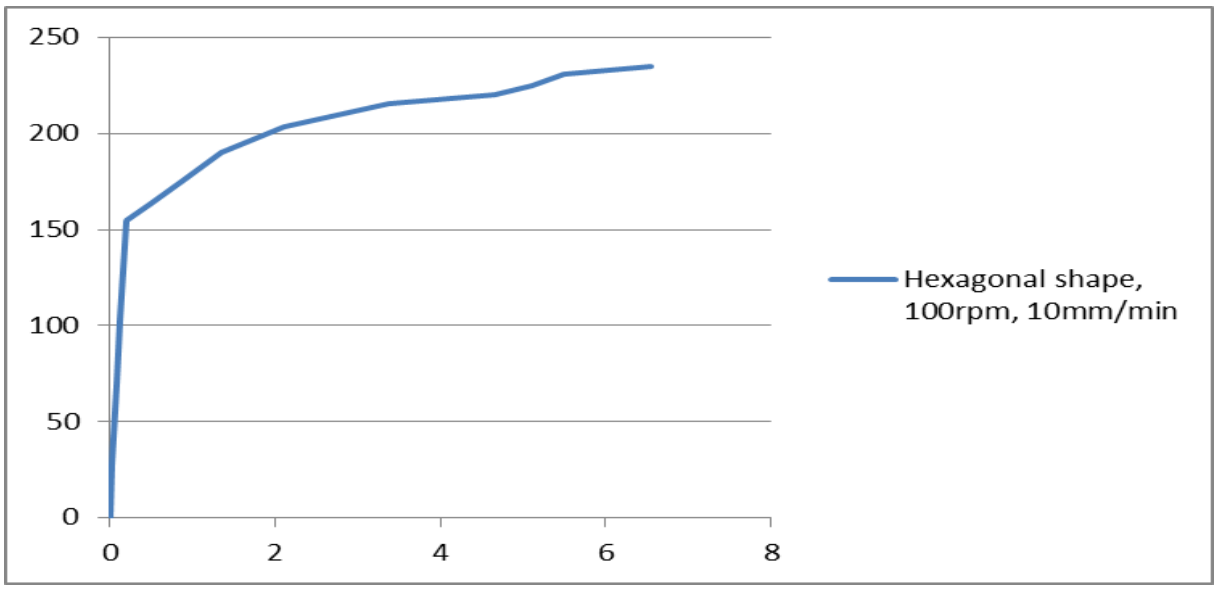

Figure 4.27 Stress Strain curve for Aluminum AA5083 and AA6061

Hexagonal shape proves to be defect free for welding, also it can be seen that rotational speed, traverse speed with probe shape plays a vital role to obtain defect free Friction stir welded parts.

CHAPTER 5: CONCLUSION & FUTURE WORK

Numerical simulation was performed for similar and dissimilar materials. Nine samples for similar materials were modeled and for dissimilar materials only one sample was modeled. Graphs obtained after modeling evaluated that the sample with square shape, 3250 rpm rotational speed and traverse speed of 200 mm/min was best as it gave highest tensile strength i.e. 183 MPa which has validated the experimental result for similar materials . Similarly for dissimilar material Hexagonal shape proves to be defect free for welding, also it can be seen that rotational speed, traverse speed with probe shape plays a vital role to obtain defect free Friction stir welded parts. Also rotational speed of 100 rpm and 10mm/min traverse speed gave tensile strength of 202 MPa which has also validated experimental data for dissimilar materials. Moreover it can be observed that Friction stir welding is highly influenced with the behavior of these three parameters. Hence best weld quality could be achieved by considering above parameters.

Experimental results can be validated by numerical simulations as it is comparatively easy and can be applied for any material. Also during modeling you can easily vary parameters in order to consider their effect easily and thus optimal values can be obtained.

It can be concluded that both thick and thin sheets can be easily modeled using any simulating software and their effects on parameters can be easily observed.

In the future, different parameters can be analyzed to evaluate temperature distribution for Friction Stir Welding numerically. Also other alloys except Aluminum can be used to observe their effect on weld strength. Pre heating effect can be considered for Friction stir welding which can be simulated using ABAQUS. Temperature distribution during FSW can be analyzed.

References:

1. Venkatesh, K. M., Arivarsu, M., Manikandan, M., & Arivazhagan, N. (2018). Review on friction stir welding of steels. *Materials Today: Proceedings*, *5*(5), 13227–13235.

2. Smolin, A. Y., Shilko, E. V., Astafurov, S. V., Kolubaev, E. A., Eremina, G. M., & Psakhie, S. G. (2018). Understanding the mechanisms of friction stir welding based on computer simulation using particles. *Defence Technology*.

3. Entesari, S., Abdollah-zadeh, A., Habibi, N., & Mehri, A. (2017). Experimental and numerical investigations into the failure mechanisms of friction stir welded AA7075-T6 thin sheets. *Journal of Manufacturing Processes*.

4. Subhashini, P. V. S., & Manas, Y. N. C. (2018). Analysis and Optimization of Parameters for Friction Stir Welding. *Materials Today: Proceedings*, *5*(5), 12376–12383.

5. Ahmad, B., Galloway, A., & Toumpis, A. (2018). Advanced numerical modelling of friction stir welded low alloy steel. *Journal of Manufacturing Processes*.

6. Ahmed, S., & Saha, P. (2018). Development and testing of fixtures for friction stir welding of thin aluminium sheets. *Journal of Materials Processing Technology*.

7. Huang, Y., Meng, X., Zhang, Y., Cao, J., & Feng, J. (2017). Micro friction stir welding of ultra-thin Al-6061 sheets. *Journal of Materials Processing Technology*. Chen, S., Li, X., Jiang, X., Yuan, T., & Hu, Y. (2018). The effect of microstructure on the mechanical properties of friction stir welded 5A06 Al Alloy. *Materials Science and Engineering A*, *735*(August), 382–393.

8. Watanabe, T., Takayama, H., & Yanagisawa, A. (2006). Joining of aluminum alloy to steel by friction stir welding. *Journal of Materials Processing Technology*, *178*(1–3), 342–349.

9. Riahi, M., & Nazari, H. (2011). Analysis of transient temperature and residual thermal stresses in friction stir welding of aluminum alloy 6061-T6 via numerical simulation. *The International Journal of Advanced Manufacturing Technology*, *55*(1–4), 143–152. Elangovan, K., & Balasubramanian, V. (2008).

10. Influences of tool pin profile and welding speed on the formation of friction stir processing zone in AA2219 aluminium alloy. *Journal of Materials Processing Technology*, *200*(1–3), 163–175.

11. Engg, M. (2008). 1 1. Dept of Mechanical Engg, K.L. College of Engg, Vaddeswaram, AP, India 2. Dept of Mech. Engg, Osmania University, Hyderabad, AP, India, *1*(2), 95–101.

12. Singh, B. (2017). Modeling and Analysis of Friction Stir Welding, *3*(2), 7–9.

13. Darras, B. M. (2005). Experimental and Analytical Study of Friction Stir Processing, 2403–2409.

14. R.S. Mishra & Z.Y. Ma. (2005) Friction Stir Welding and processing, 1-78.

15. Materials and Processes in Manufacturing by E. Paul DeGarmo, J.T. Black, and Ronald A. Kosher

16. Bull, Steve (March 16, 2000), "Fusion Welding Processes", MMM373 Joining Technology course website, Newcastle upon Tyne, England, United Kingdom: Newcastle University School of Chemical Engineering and Advanced Materials, archived from the original on September 11, 2007, retrieved May 16, 2010

17. Parkinson, A.R., R.J. Balling, and J.D. Hedengren, Optimization Methods for Engineering Design Applications and Theory2013.

18. Rawal, M.R. and K. H.Inamdar, Review on Various Optimization Techniques used for Process Parameters of Resistance Spot Welding. International Journal of Current Engineering and Technology, 2014.

19. Sagheer-Abbasi, Y., Ikramullah-Butt, S., Hussain, G., Imran, S. H., Mohammad-Khan, A., & Baseer, R. A. (2019). Optimization of parameters for micro friction stir welding of aluminum 5052 using Taguchi technique. International Journal of Advanced Manufacturing Technology, 102(1–4), 369–378.

20. Jalili, N., Basirat Tabrizi, H., & Hosseini, M. M. (2016).). Experimental and numerical study of simultaneous cooling with CO2 gas during friction stir welding of Al-5052. Journal of Materials Processing Technology, 237, 243–253.

21. Experimental and numerical study of simultaneous cooling with CO2 gas during friction stir welding of Al-5052. Journal of Materials Processing Technology, 237, 243–253.

22. Hariharan, K., Lee, M. G., Kim, M. J., Han, H. N., Kim, D., & Choi, S. (2015). Decoupling Thermal and Electrical Effect in an Electrically Assisted Uniaxial Tensile Test Using Finite Element Analysis. Metallurgical and Materials Transactions A: Physical Metallurgy and Materials Science, 46(7), 3043–3051.

23. Saad Khalid. Friction Stir Welding of Dissimilar Aluminum alloys, Master thesis, National University of Science & Technology, 2018

24. Zhang, Y., Yi, Y., Huang, S., & He, H. (2017). Influence of Temperature-Dependent Properties of Aluminum Alloy on Evolution of Plastic Strain and Residual Stress during Quenching Process. Metals, 7(6), 228.

25. Kim, D., Badarinarayan, H., Kim, J. H., Kim, C., Okamoto, K., Wagoner, R. H., & Chung, K. (2010). Numerical simulation of friction stir butt welding process for AA5083-H18 sheets. European Journal of Mechanics, A/Solids, 29(2), 204–215.

26. Clausen, A. H., Børvik, T., Hopperstad, O. S., & Benallal, A. (2004). Flow and fracture characteristics of aluminium alloy AA5083-H116 as function of strain rate, temperature and triaxiality. Materials Science and Engineering A, 364(1–2), 260–272.